Simulation of liver cancer treatment using ^{90}Y microspheres based on anatomical image segmentation technique and Geant4 toolkit

Speaker: Ha Nguyen Hong

QuyNhon, August 2019

- Motivation
- Research objectives
- Materials and methods

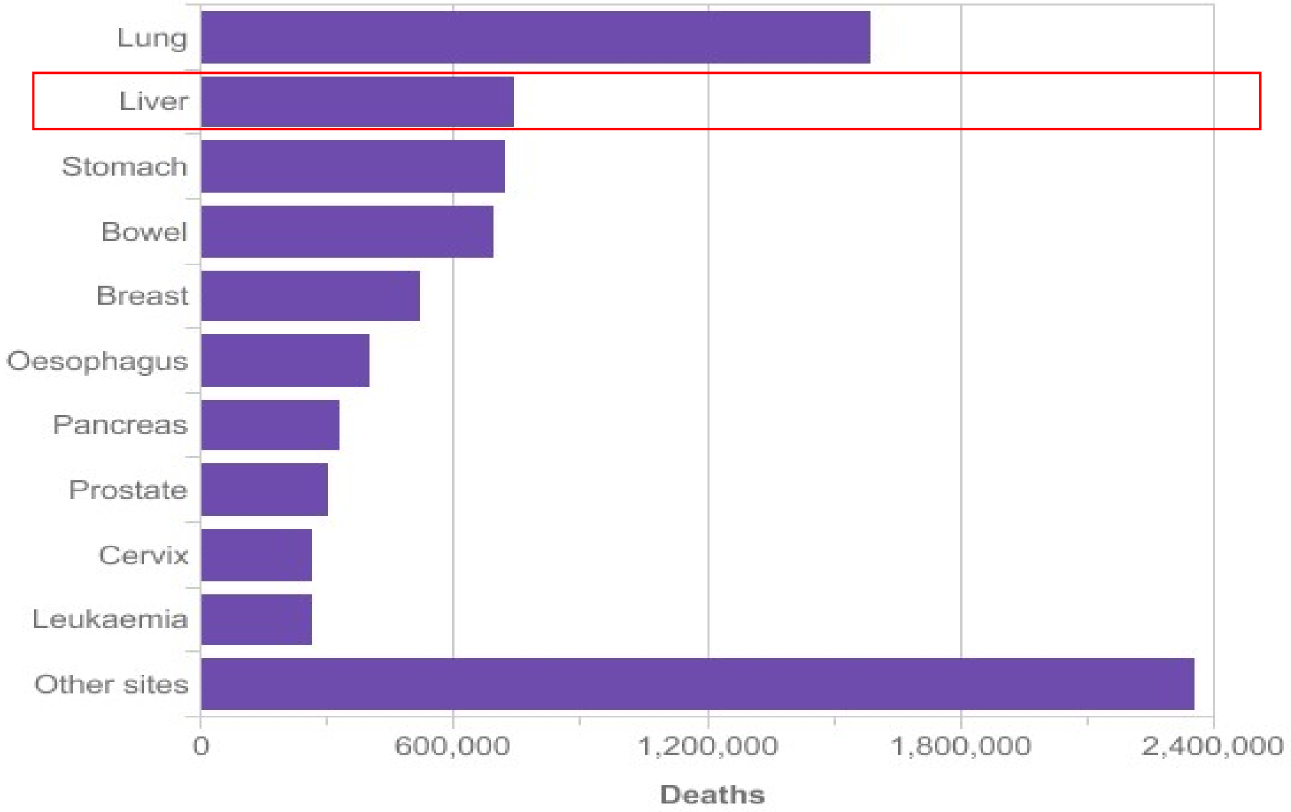

The 10 Most Common Causes of Cancer Death, World, 2012 Estimates

Worldwide cancer statistics – Cancer Research UK

❑ Treatment techniques

- Surgery
- Chemotherapy
- **Radioembolization** (with ^{90}Y microspheres)

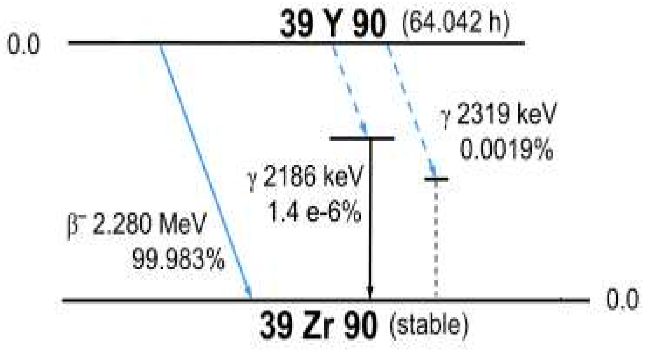

^{90}Y: Pure-beta emitter;
$E_{\beta max}$ = 2.28 MeV;
beta-penetration depth in tissue: 11.4 mm

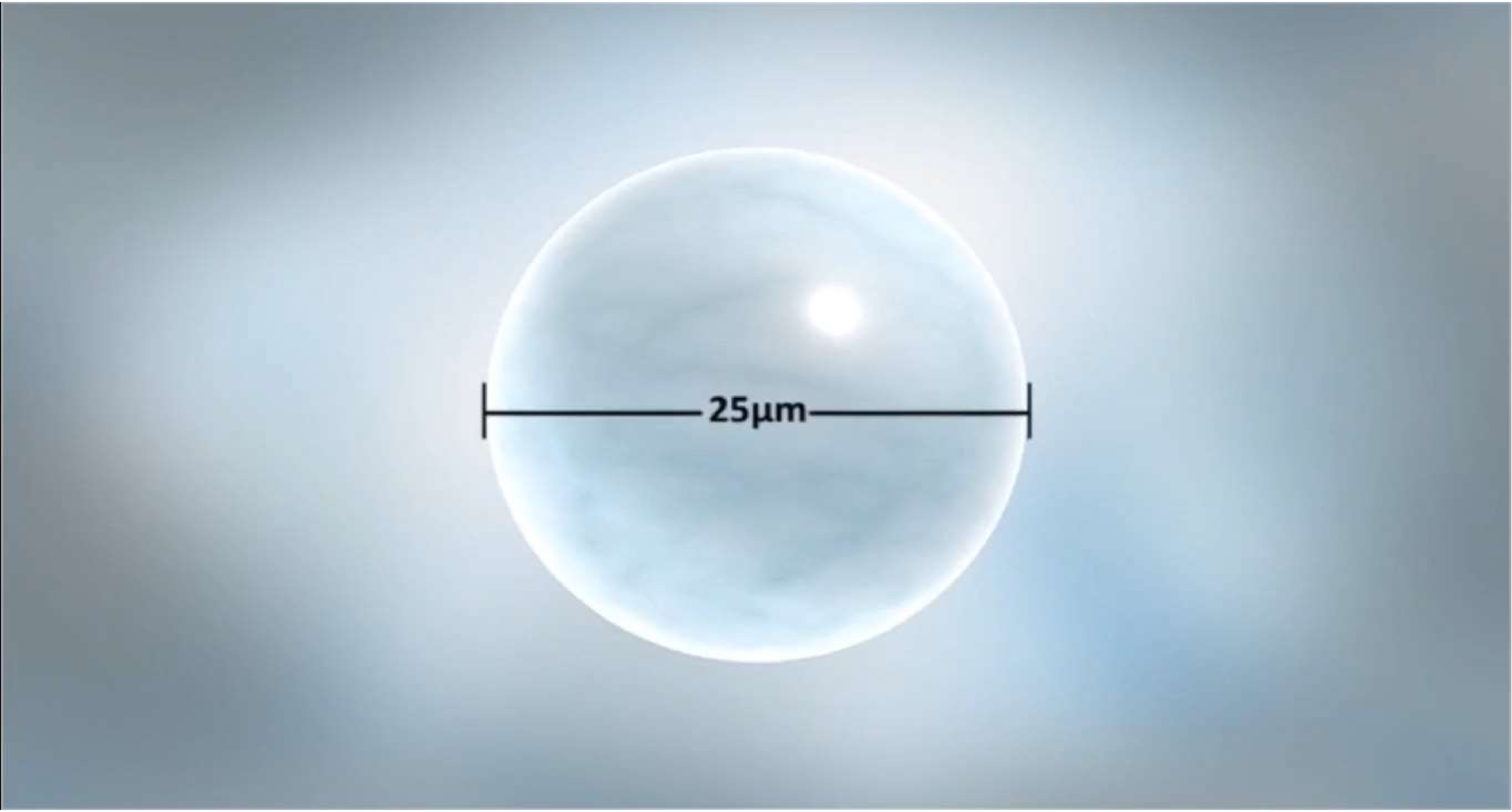

Source: SIRTex

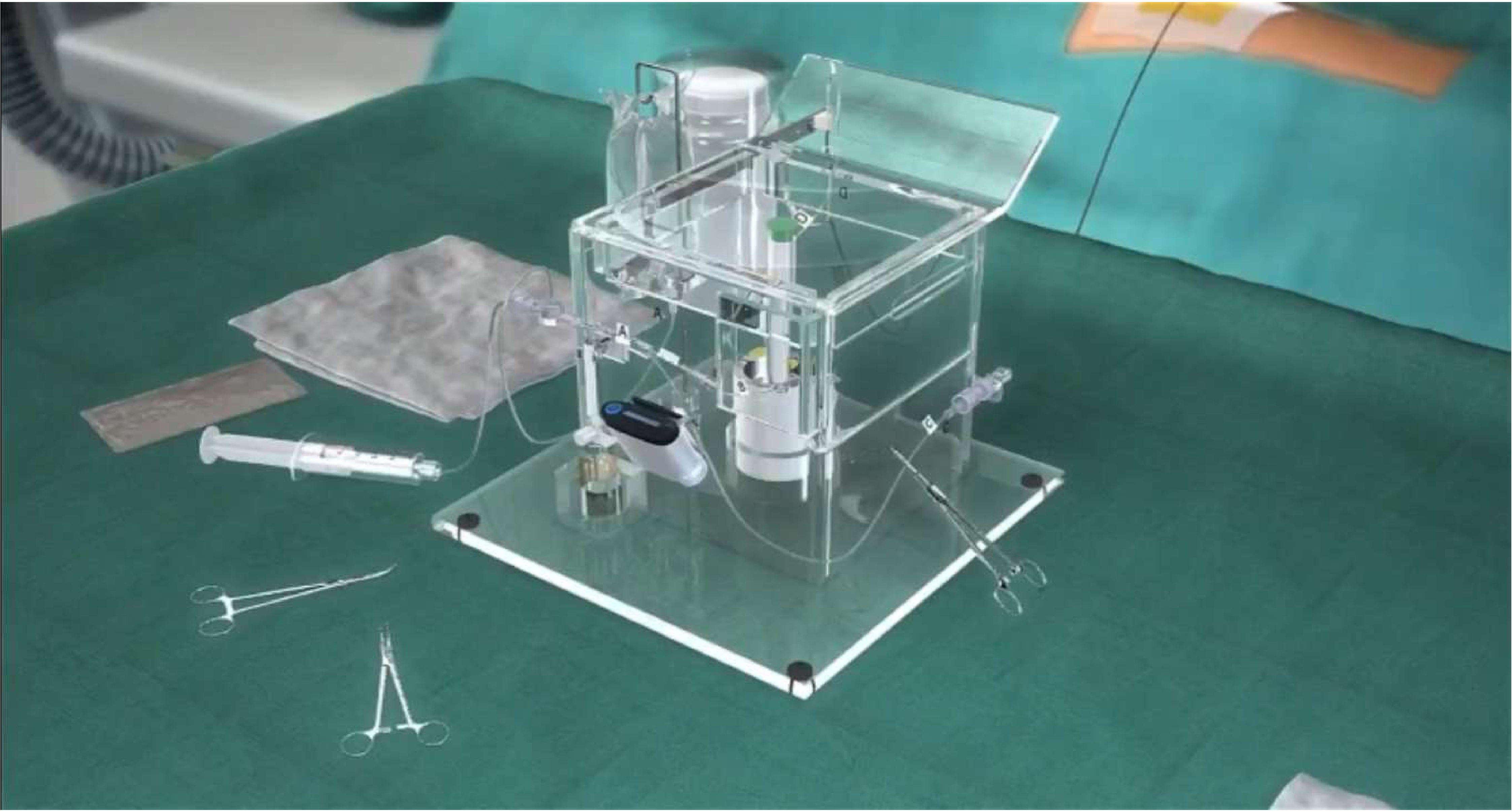

Source: SIRTex

Radioembolization with ^{90}Y

☐ STEPS TO IMPLEMENT

1. Clinical examination

2. Pre-treatment

- CT and SPECT scan
- Using ^{99m}Tc-MAA (Macroaggregated albumin) through microcatheter
- Calculate lungs shunt fraction (LSF)

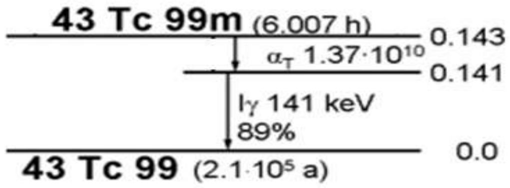

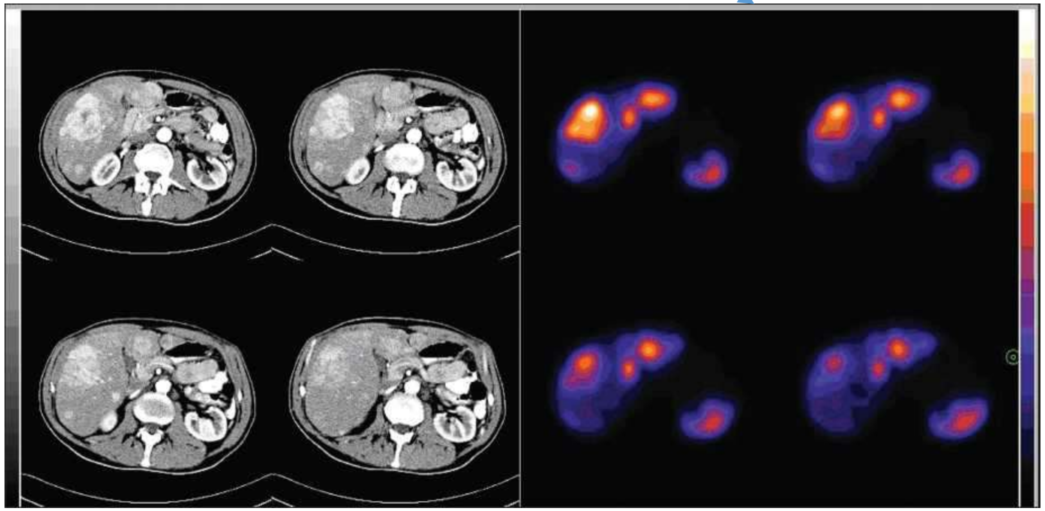

3. Activity planning of ^{90}Y

- BSA; Partition model; MIRD methods.

4. Treatment

1. Empiric Method Calculation:

Tumor ≤ 25 % of the liver mass → 2 GBq for whole liver

Tumor >25% but <50 % of the liver mass → 2.5 GBq for whole liver

Tumor >50 % of liver mass → 3 GBq for whole liver

2. Body Surface Area (BSA) Method Calculation :

$$\boxed{\mathrm{BSA}\left[\mathrm{m}^2\right] = 0.20247 \times (\mathrm{height}[\mathrm{m}])^{0.725} \times (\mathrm{weight}[\mathrm{kg}])^{0.425}} \tag{1}$$

$$\boxed{\mathrm{A}[\mathrm{GBq}] = (\mathrm{BSA} - 0.2) + \frac{\text{vol of tumor}}{\text{vol of tumor} + \text{vol of liver}}} \tag{2}$$

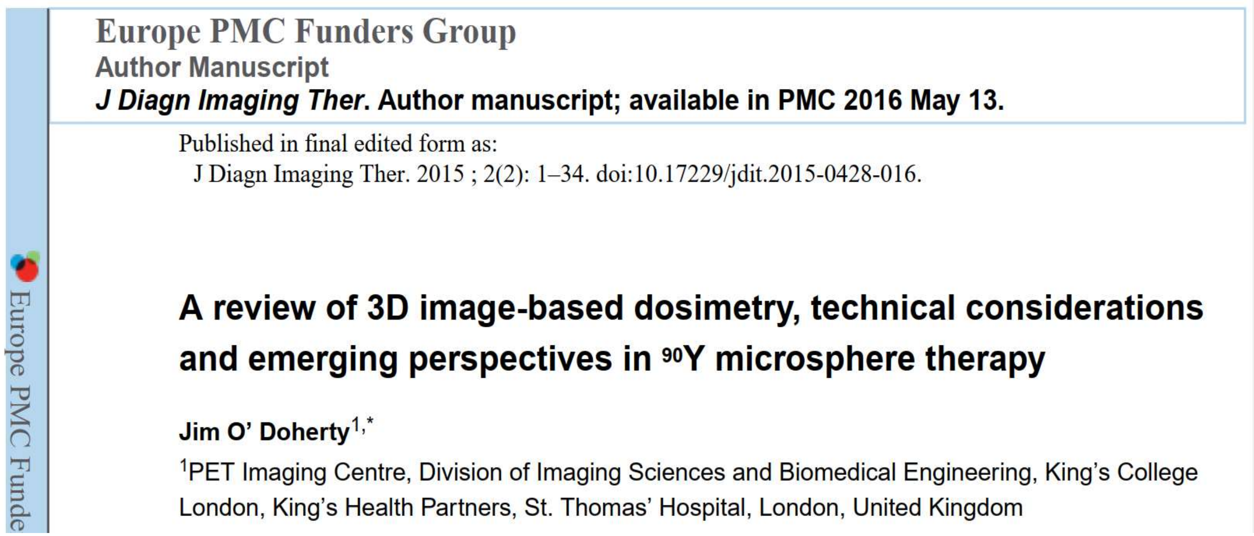

J Diagn Imaging Ther. Author manuscript; available in PMC 2016 May 13.

Published in final edited form as:
J Diagn Imaging Ther. 2015 ; 2(2): 1–34. doi:10.17229/jdit.2015-0428-016.

A review of 3D image-based dosimetry, technical considerations and emerging perspectives in ^{90}Y microsphere therapy

Jim O' Doherty[1,*]

[1]PET Imaging Centre, Division of Imaging Sciences and Biomedical Engineering, King's College London, King's Health Partners, St. Thomas' Hospital, London, United Kingdom

J Diagn Imaging Ther. 2015 ; 2(2): 1–34. DOI:10.17229/jdit.2015-0428-016

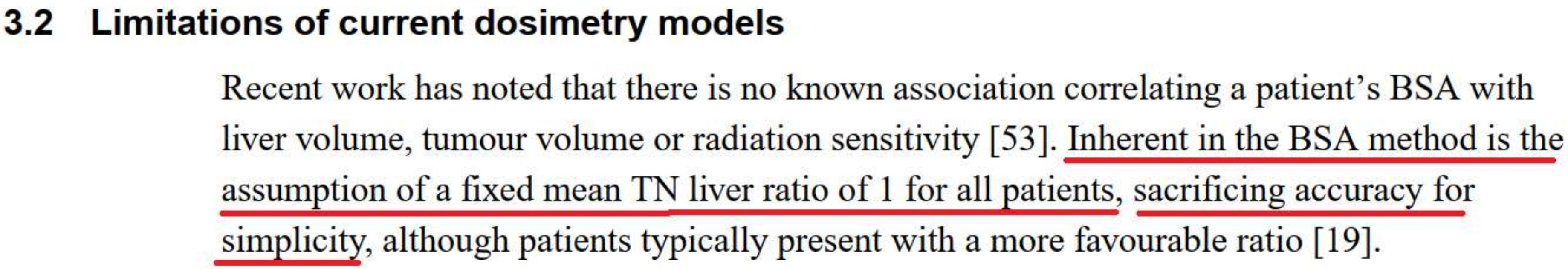

3.2 Limitations of current dosimetry models

Recent work has noted that there is no known association correlating a patient's BSA with liver volume, tumour volume or radiation sensitivity [53]. Inherent in the BSA method is the assumption of a fixed mean TN liver ratio of 1 for all patients, sacrificing accuracy for simplicity, although patients typically present with a more favourable ratio [19].

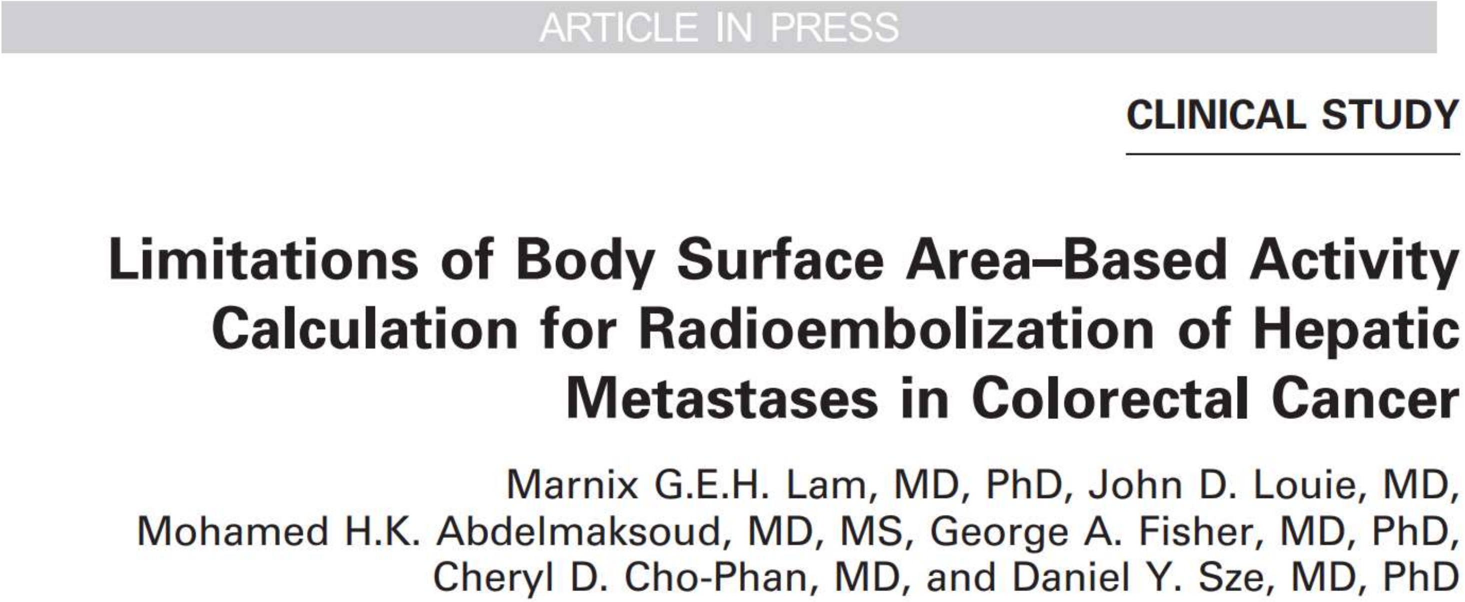

ARTICLE IN PRESS

CLINICAL STUDY

Limitations of Body Surface Area–Based Activity Calculation for Radioembolization of Hepatic Metastases in Colorectal Cancer

Marnix G.E.H. Lam, MD, PhD, John D. Louie, MD,
Mohamed H.K. Abdelmaksoud, MD, MS, George A. Fisher, MD, PhD,
Cheryl D. Cho-Phan, MD, and Daniel Y. Sze, MD, PhD

J Vasc Interv Radiol. 2014 Jul;25(7):1085-93.

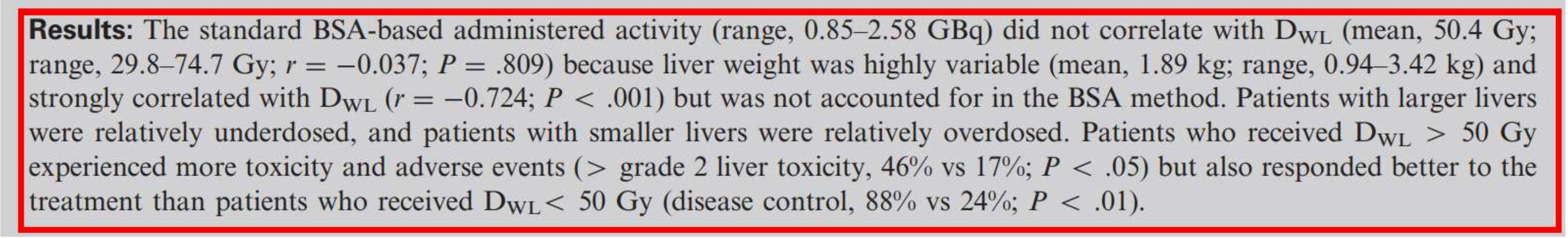

Results: The standard BSA-based administered activity (range, 0.85–2.58 GBq) did not correlate with D_{WL} (mean, 50.4 Gy; range, 29.8–74.7 Gy; $r = -0.037$; $P = .809$) because liver weight was highly variable (mean, 1.89 kg; range, 0.94–3.42 kg) and strongly correlated with D_{WL} ($r = -0.724$; $P < .001$) but was not accounted for in the BSA method. Patients with larger livers were relatively underdosed, and patients with smaller livers were relatively overdosed. Patients who received $D_{WL} > 50$ Gy experienced more toxicity and adverse events ($>$ grade 2 liver toxicity, 46% vs 17%; $P < .05$) but also responded better to the treatment than patients who received $D_{WL} < 50$ Gy (disease control, 88% vs 24%; $P < .01$).

3. Partition Model Calculation

$$\boxed{A_{\text{total -lung}} = \frac{D_{\text{lung}} \times M_{\text{lung}} \times LSF}{49670}} \qquad (3)$$

$$\boxed{A_{\text{total -normal liver}} = \frac{D_{\text{normal liver}} \times (M_{\text{normal liver}} + T{:}N \times M_{\text{tumor}})}{49670 \times (1 - LSF)}} \qquad (4)$$

$$T{:}N = (A_{\text{tumor}} / M_{\text{tumor}}) / (A_{\text{normal liver}} / M_{\text{normal liver}}) \qquad (5)$$

D_{lung}: Limiting lung dose – 25Gy

$D_{\text{normal liver}}$: Limiting normal liver dose – 80 Gy
(70 Gy for patients with cirrhosis)

LSF: Lungs shunt fraction (%)

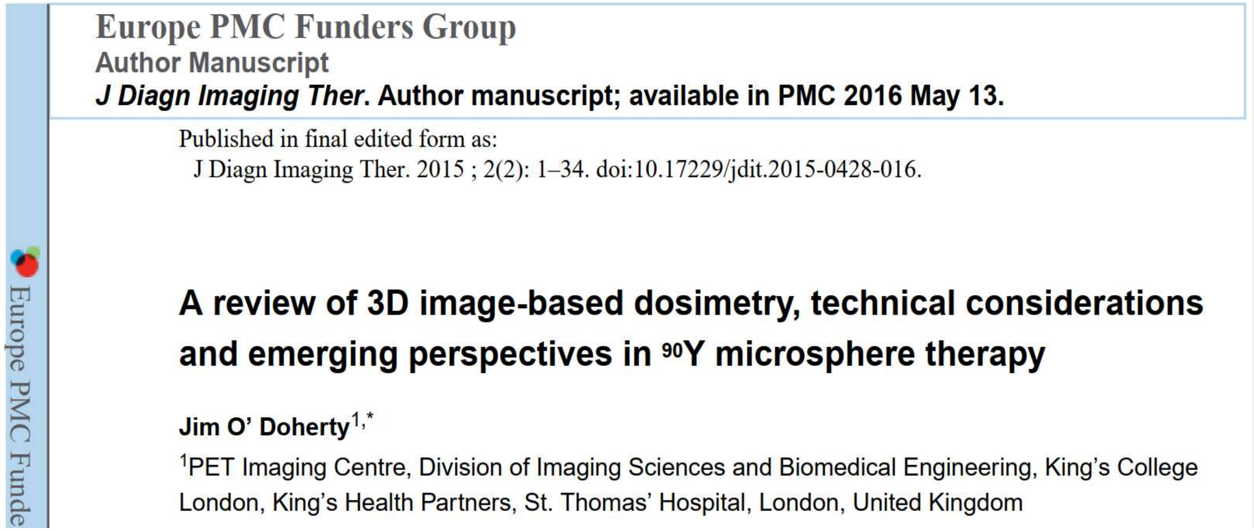

Published in final edited form as:
J Diagn Imaging Ther. 2015 ; 2(2): 1–34. doi:10.17229/jdit.2015-0428-016.

A review of 3D image-based dosimetry, technical considerations and emerging perspectives in ^{90}Y microsphere therapy

Jim O' Doherty[1,*]
[1]PET Imaging Centre, Division of Imaging Sciences and Biomedical Engineering, King's College London, King's Health Partners, St. Thomas' Hospital, London, United Kingdom

J Diagn Imaging Ther. 2015 ; 2(2): 1–34. doi:10.17229/jdit.2015-0428-016

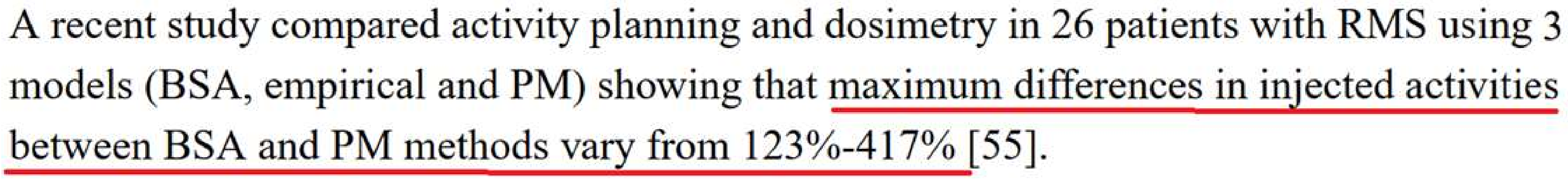

A recent study compared activity planning and dosimetry in 26 patients with RMS using 3 models (BSA, empirical and PM) showing that maximum differences in injected activities between BSA and PM methods vary from 123%-417% [55].

MIRD Method:

MIRD Pamphlet 5 mathematical phantom

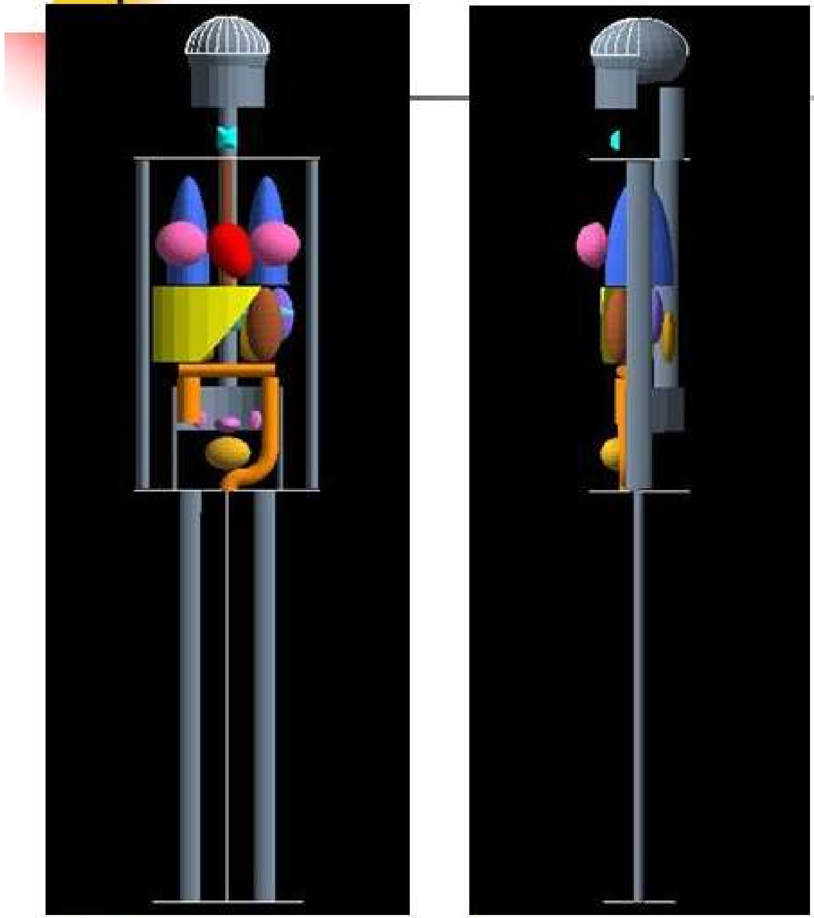

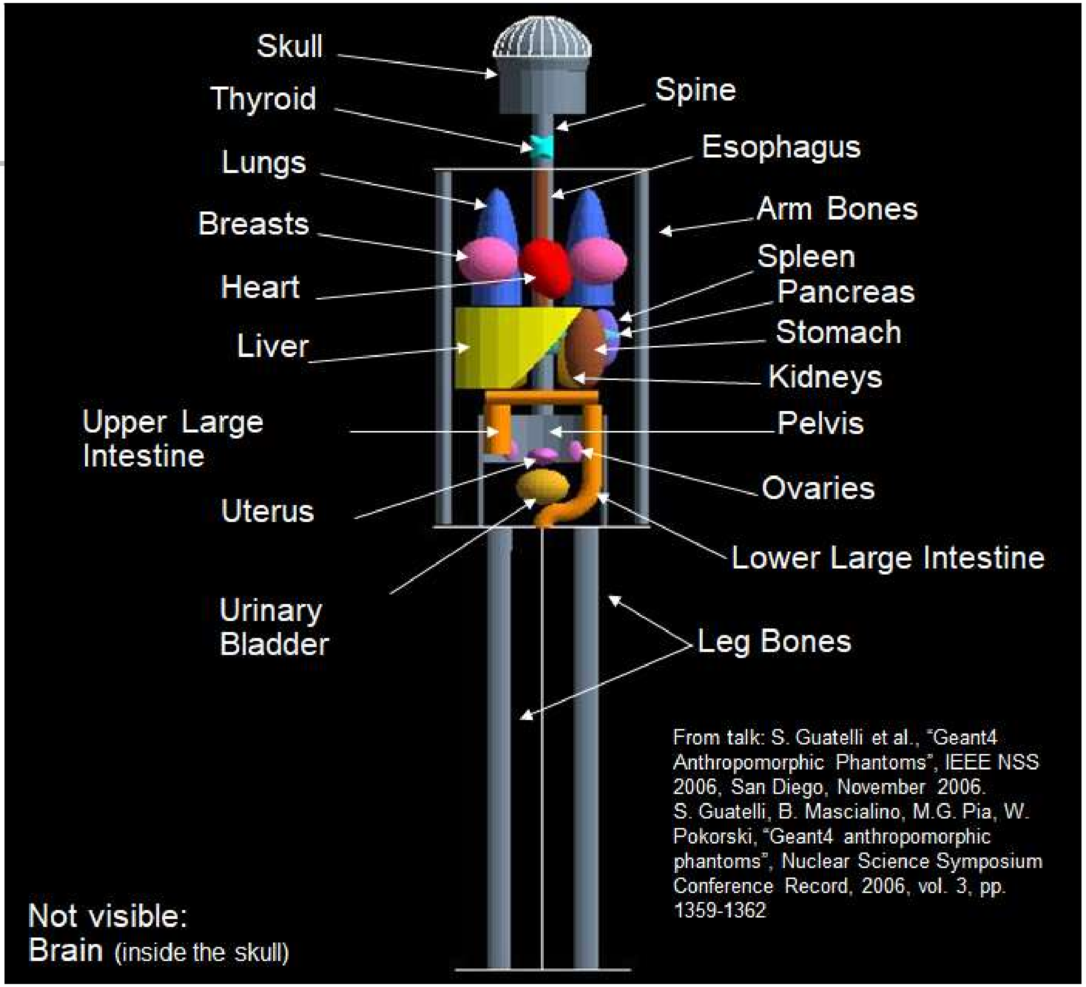

From talk: S. Guatelli et al., "Geant4 Anthropomorphic Phantoms", IEEE NSS 2006, San Diego, November 2006.
S. Guatelli, B. Mascialino, M.G. Pia, W. Pokorski, "Geant4 anthropomorphic phantoms", Nuclear Science Symposium Conference Record, 2006, vol. 3, pp. 1359-1362

Not visible:
Brain (inside the skull)

Research objective

❑ STEPS TO IMPLEMENT

1. Clinical examination

2. Pre-treatment

- CT and SPECT scan
- Using ^{99m}Tc-MAA (Macroaggregated albumin) through microcatheter
- Calculate lungs shunt fraction (LSF)

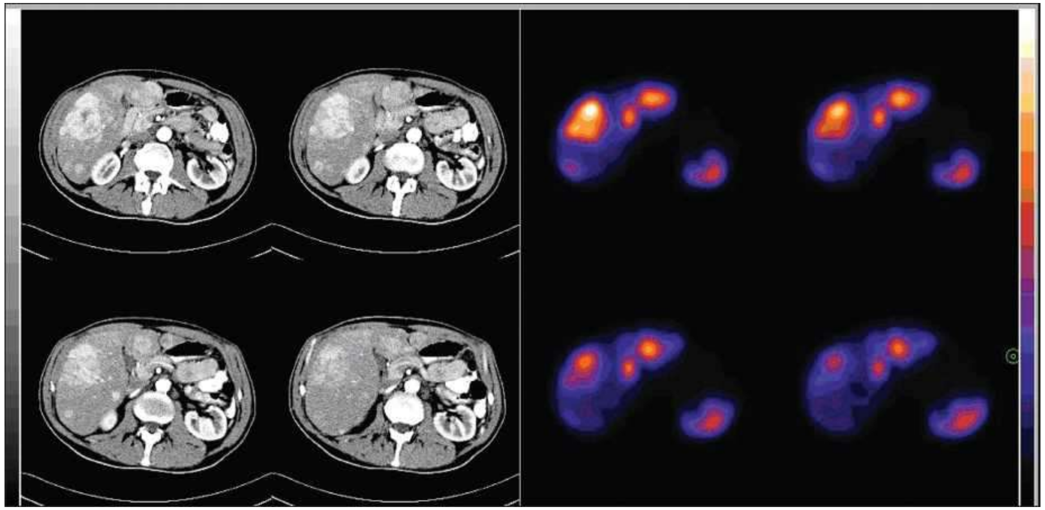

3. Activity planning of ^{90}Y

- BSA; Partition model; MIRD methods.

➡ Image-based simulation method

4. Treatment

OEDIPE - Outil d’Evaluation de la Dose Interne PErsonnalisée

- Based on MCNPX
- Simulated on human voxel model and ORNL mathematical model


(a) (b)

Figure 2. Two-dimensional voxel-based representation of the liver and kidneys of the adult ORNL model with two voxel sampling sizes: $1.58 \times 1.58 \times 5$ mm^3 (a) and $3.16 \times 3.16 \times 5$ mm^3 (b).

Table 4. Parameters to study the effect of voxel sampling and voxel size.

Geometry	Adult ORNL model	Adult ORNL model	Adult ORNL model
Geometry definition	Mathematical	Voxel-based $1.58 \times 1.58 \times 5$ mm^3	Voxel-based $3.16 \times 3.16 \times 5$ mm^3
Calculation method	Monte Carlo	Monte Carlo	Monte Carlo
Calculation code	MCNPX2.5e	MCNPX2.5e	MCNPX2.5e

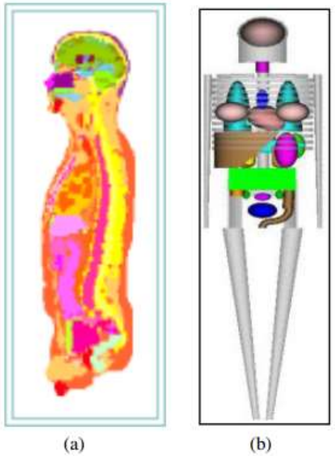
(a) (b)

Figure 1. Voxel-based Zubal model (a) and the standard adult ORNL mathematical model (b). (This figure is in colour only in the electronic version)

Table 1. Oedipe interface validation parameters.

	SCMS (Yoriyaz)	Oedipe
Geometry	Zubal	Zubal
Geometry definition	Voxel-based	Voxel-based
Calculation method	Monte Carlo	Monte Carlo
Calculation code	MCNP4B	MCNPX2.5e

Table 2. Study parameters for the calculation of Monte Carlo codes specificities.

	Petoussi-Henß	Oedipe
Geometry	Zubal	Zubal
Geometry definition	Voxel-based	Voxel-based
Calculation method	Monte Carlo	Monte Carlo
Calculation code	GSF code	MCNPX2.5e

Validation of a personalized dosimetric evaluation tool (Oedipe) for targeted radiotherapy

VIDA toolkit

- Based on Geant4

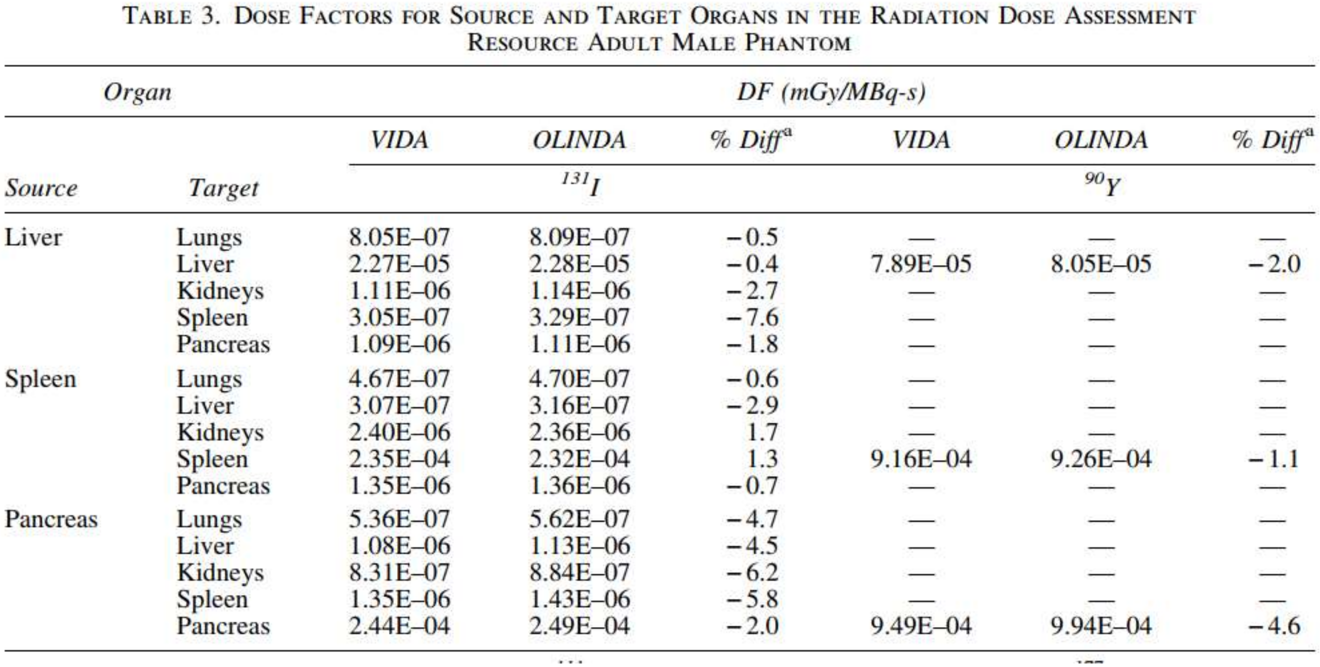

TABLE 3. DOSE FACTORS FOR SOURCE AND TARGET ORGANS IN THE RADIATION DOSE ASSESSMENT RESOURCE ADULT MALE PHANTOM

Organ		*DF (mGy/MBq-s)*					
		VIDA	*OLINDA*	*% Diff*[a]	*VIDA*	*OLINDA*	*% Diff*[a]
Source	*Target*		^{131}I			^{90}Y	
Liver	Lungs	8.05E–07	8.09E–07	−0.5	—	—	—
	Liver	2.27E–05	2.28E–05	−0.4	7.89E–05	8.05E–05	−2.0
	Kidneys	1.11E–06	1.14E–06	−2.7	—	—	—
	Spleen	3.05E–07	3.29E–07	−7.6	—	—	—
	Pancreas	1.09E–06	1.11E–06	−1.8	—	—	—
Spleen	Lungs	4.67E–07	4.70E–07	−0.6	—	—	—
	Liver	3.07E–07	3.16E–07	−2.9	—	—	—
	Kidneys	2.40E–06	2.36E–06	1.7	—	—	—
	Spleen	2.35E–04	2.32E–04	1.3	9.16E–04	9.26E–04	−1.1
	Pancreas	1.35E–06	1.36E–06	−0.7	—	—	—
Pancreas	Lungs	5.36E–07	5.62E–07	−4.7	—	—	—
	Liver	1.08E–06	1.13E–06	−4.5	—	—	—
	Kidneys	8.31E–07	8.84E–07	−6.2	—	—	—
	Spleen	1.35E–06	1.43E–06	−5.8	—	—	—
	Pancreas	2.44E–04	2.49E–04	−2.0	9.49E–04	9.94E–04	−4.6

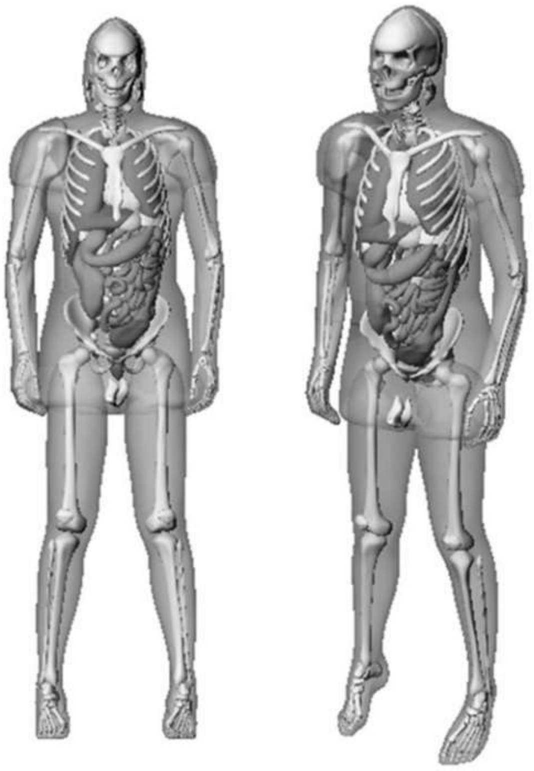

FIG. 3. Anterior views of the RADAR adult male NURBS phantom. NURBS, Non-Uniform Rational B-Spline; RADAR, Radiation Dose Assessment Resource.

VIDA: A Voxel-Based Dosimetry Method for Targeted Radionuclide Therapy Using Geant4

3D-RD toolkit

- Based on EGSnrc , extension of prior dosimetry package **3D-ID**
- Images input: SPECT, PET, CT

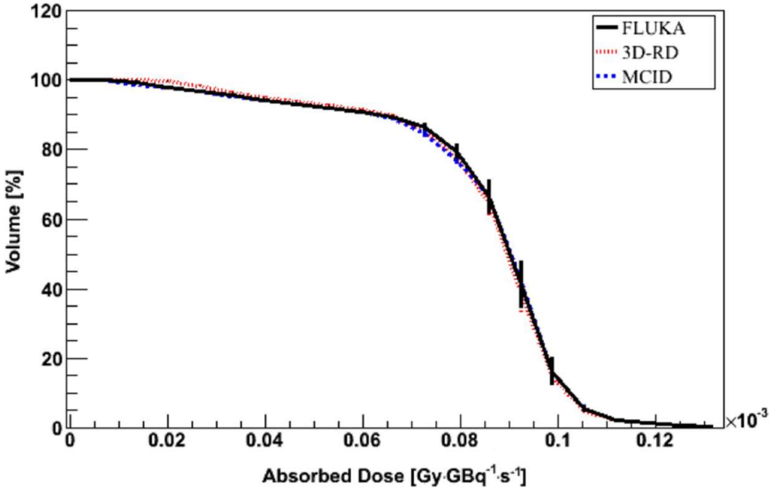

Figure 4. DVH comparison between FLUKA, 3D-RD and MCID DMC simulation in water for a VOI including a hot sphere in the PET_1 phantom. Error bars represent 1 sigma uncertainty; when not visible, they are fully included in the lines.

MCID - MC integration Internal Dosimetric (based on MCNP5)

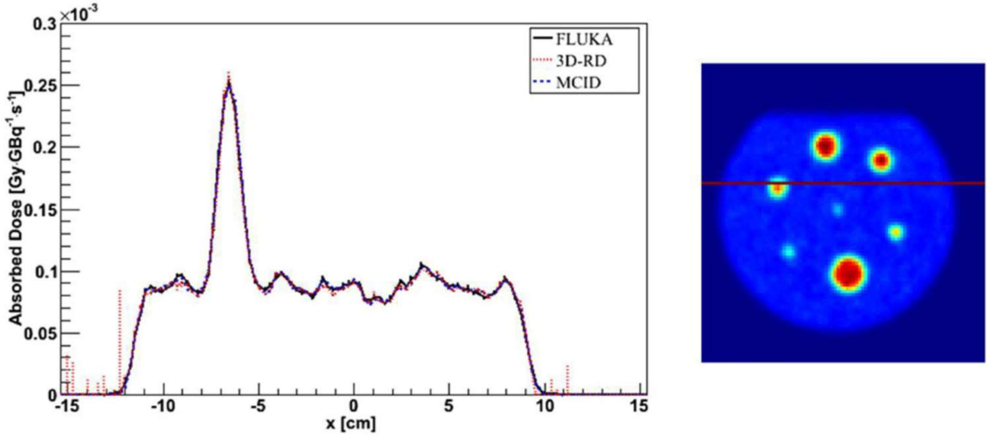

Figure 3. Profile comparison between FLUKA, 3D-RD and MCID DMC simulation in water (PET_1 phantom). Error bars are not visible because they are fully included in the lines, except for the region outside the phantom (at the profile edges) exhibiting low statistic.

Use of the FLUKA Monte Carlo code for 3D patient-specific dosimetry on PET-CT and SPECT-CT images

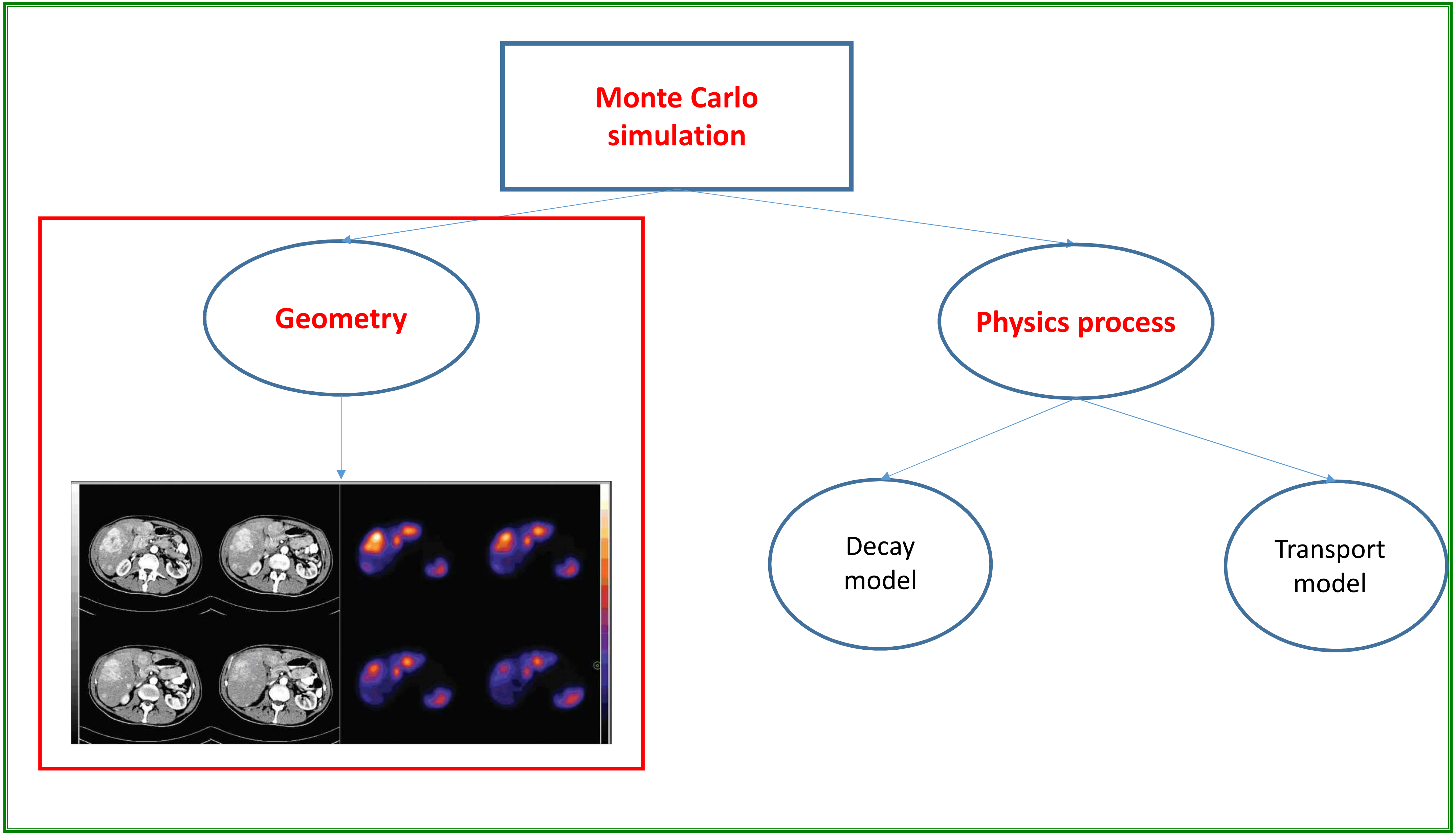
Monte Carlo simulation
Geometry
Physics process
Decay model
Transport model

Materials and methods

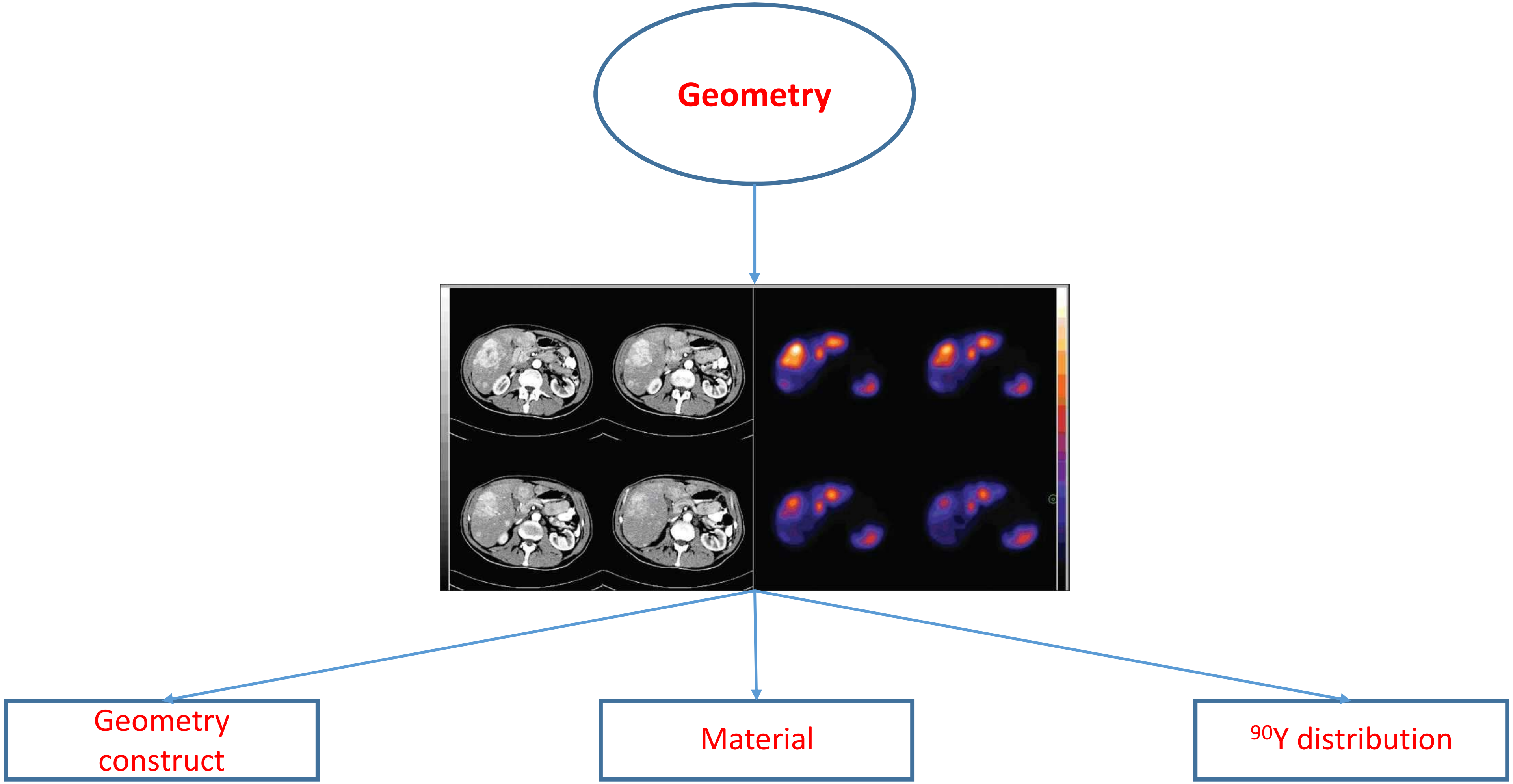

Geometry

Geometry construct

Material

^{90}Y distribution

Materials and methods

Geometry

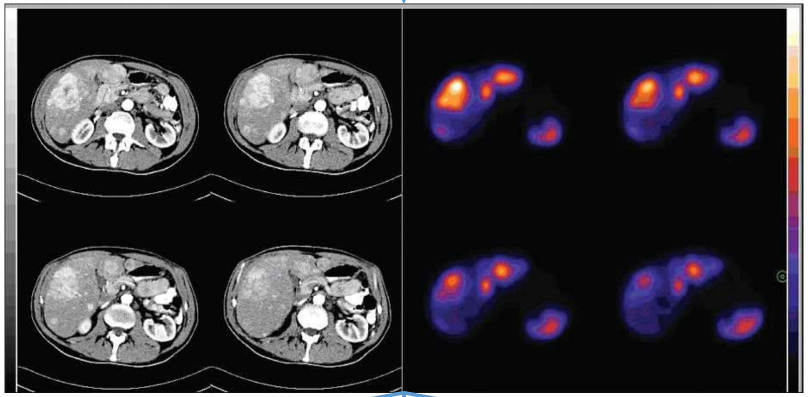

Geometry construct

Material

^{90}Y distribution

Materials and methods

Geometry construct

Individual 3D imaging (e.g., CT)

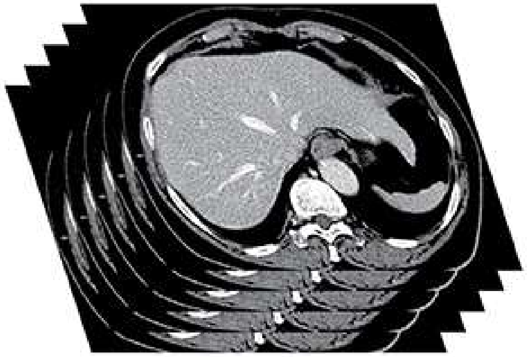

- Segmentation
- Edge detection
- 3D reconstruction

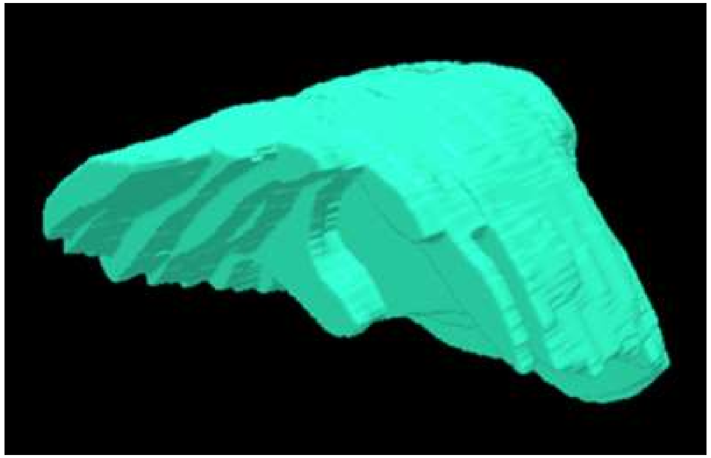

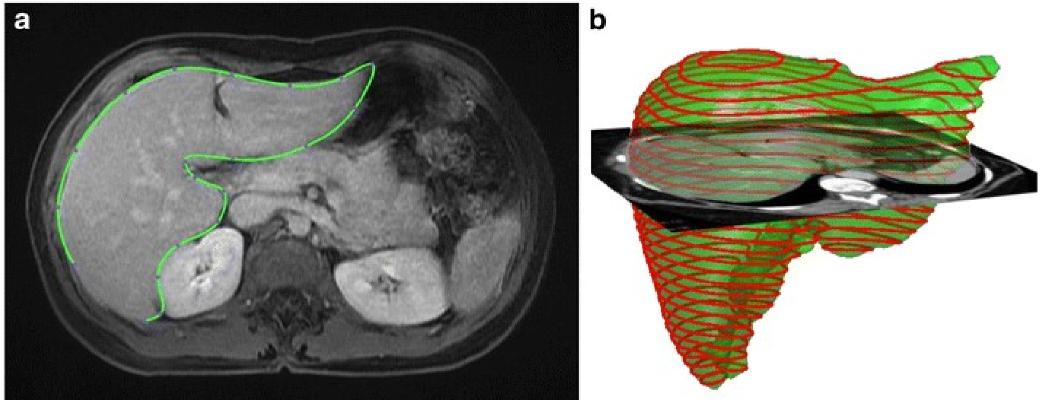

How to validate?

Materials and methods

Geometry

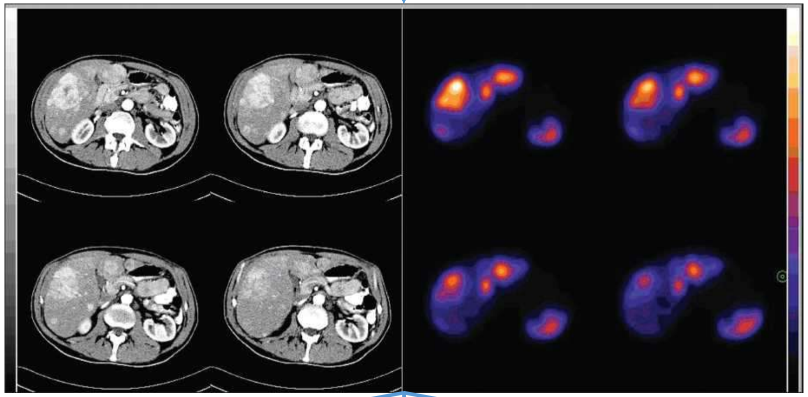

Geometry construct

Material

^{90}Y distribution

Materials and methods

Material

Electron Density Phantom model M062M

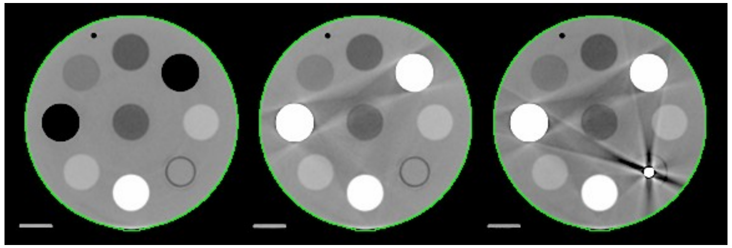

CT numbers

HU Fidelity of the AquilionLB:
https://www.wienkav.at/kav/kfj/91033454/physik/ct/edens.htm

Materials and methods

Material

CT number-density

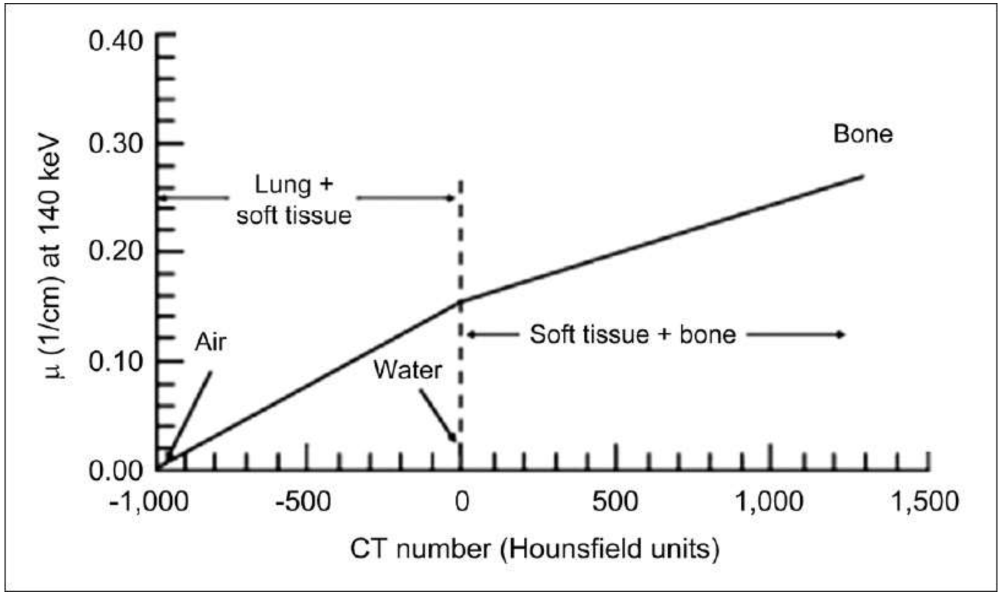

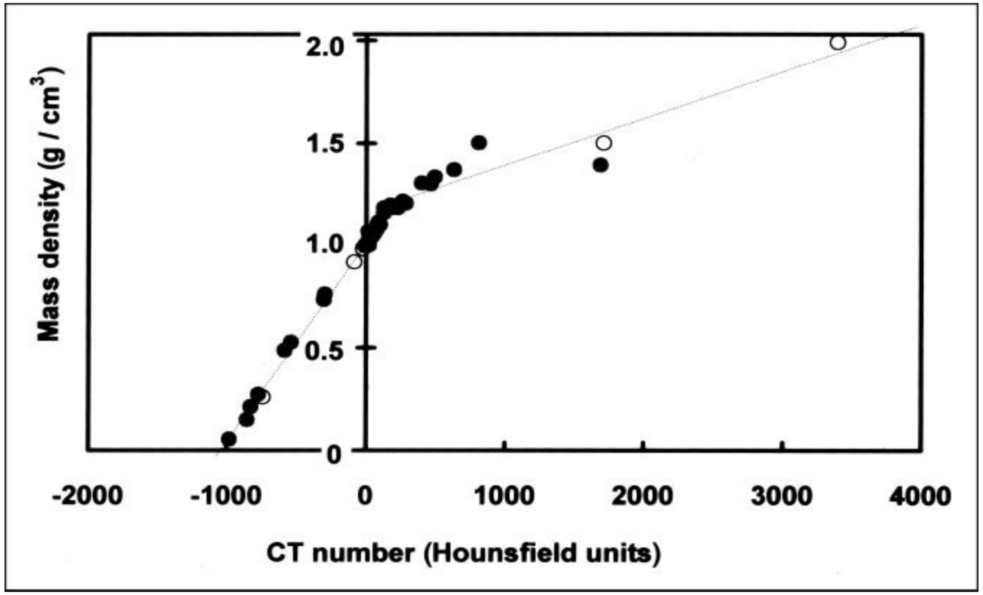

How to validate?

Materials and methods

Geometry

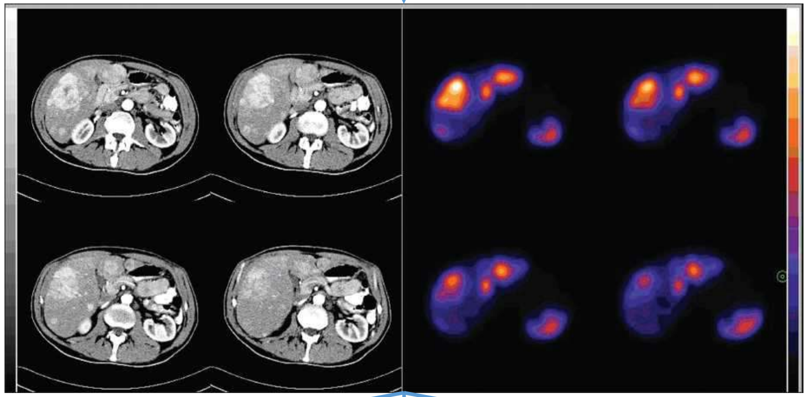

Geometry construct

Material

^{90}Y distribution

Materials and methods

^{90}Y distribution

Using SPECT image

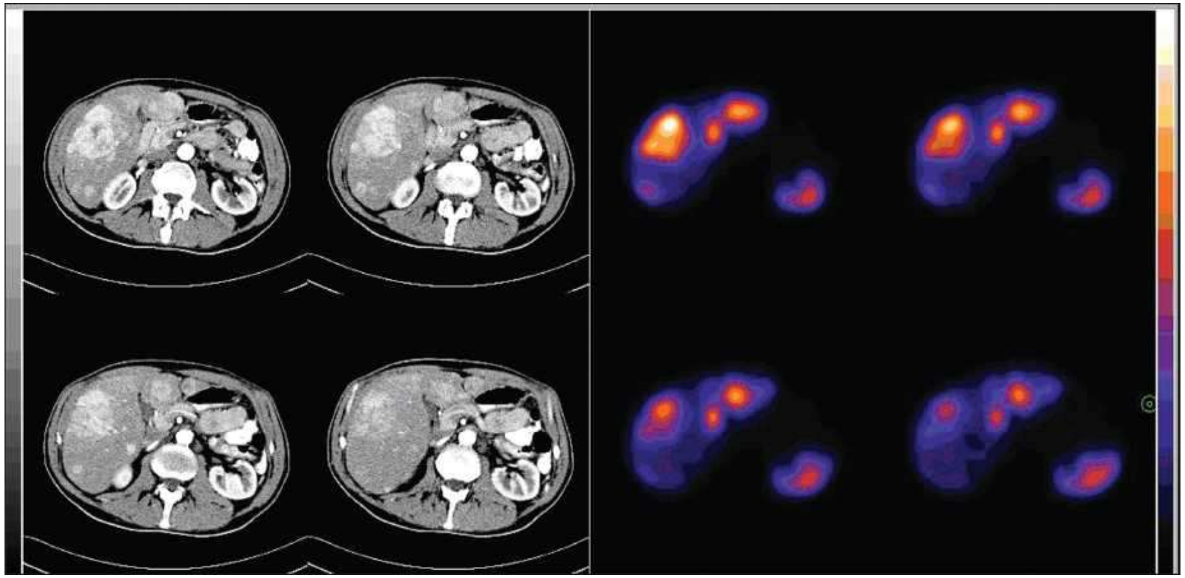

^{99m}Tc-MAA SPECT imaging

Using SPECT-CT image

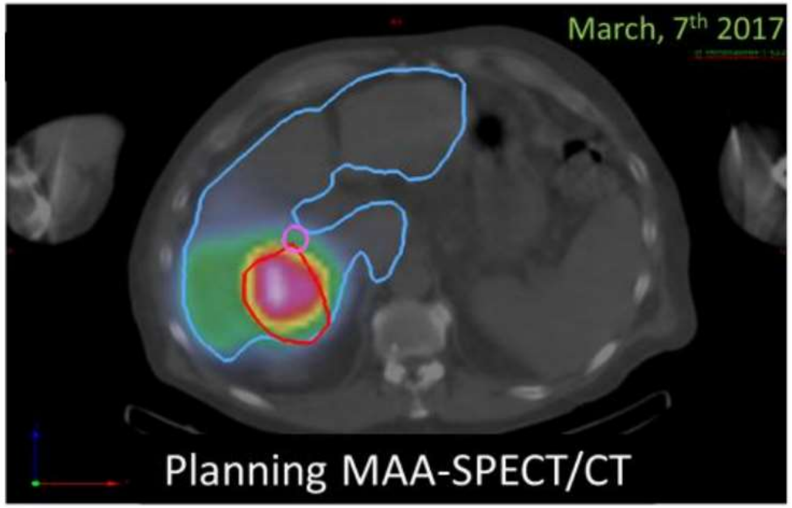

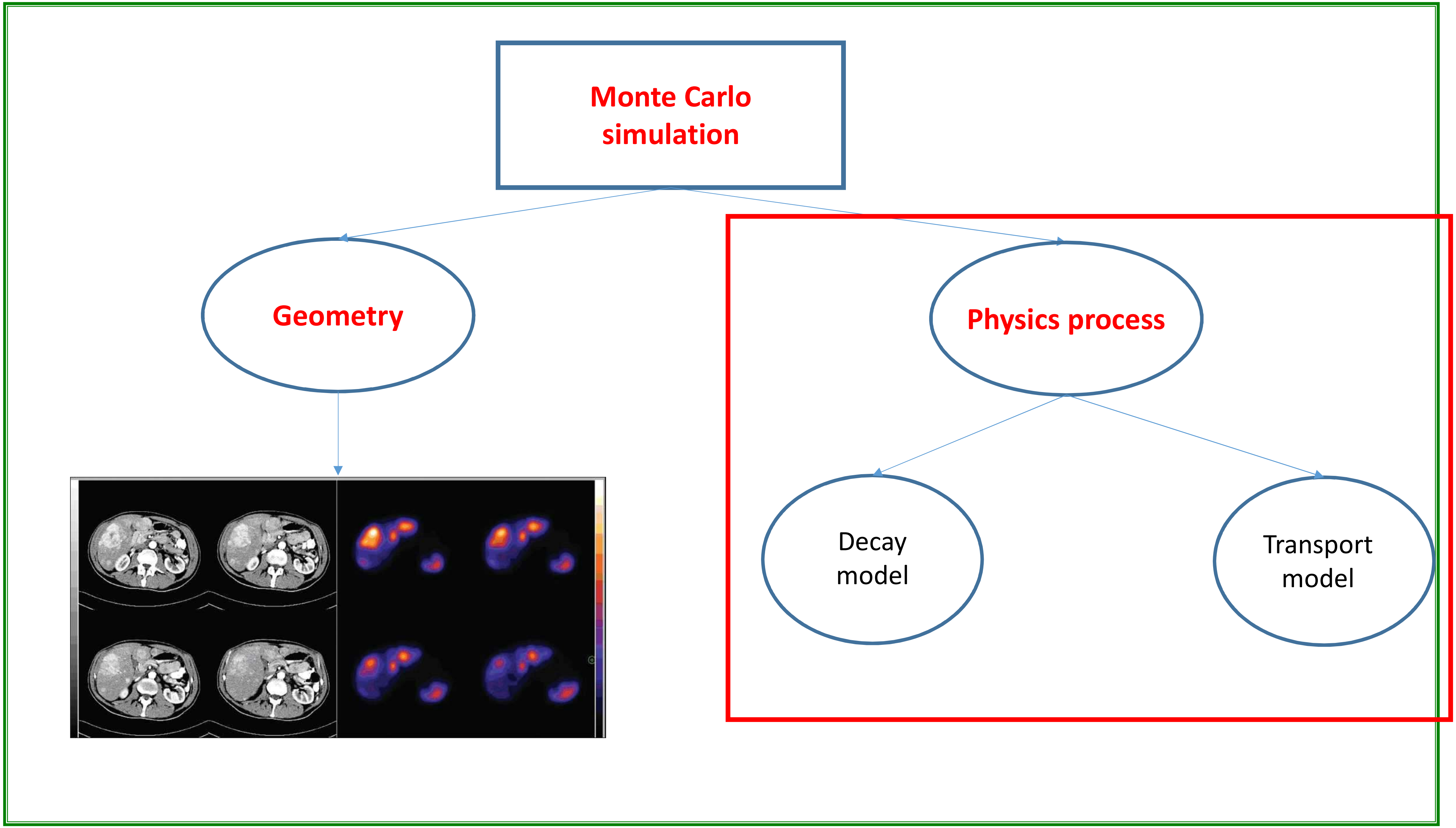

Monte Carlo simulation

Geometry

Physics process

Decay model

Transport model

Materials and methods

Geant4, an most advance OOP toolkit for the simulation of the passage of particles through matter. Its areas of application include high energy, nuclear and accelerator physics, **as well as studies in medical physics**

Geant 4 Medical applications

PET, SPECT

Courtesy of GATE Collaboration

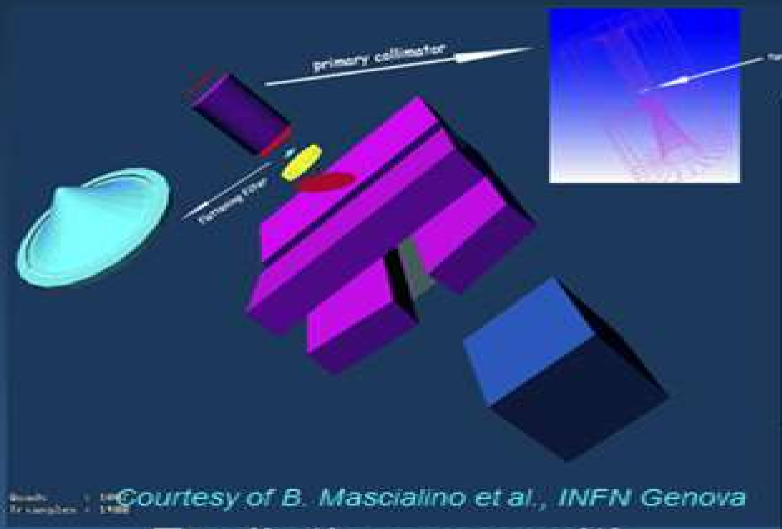

Courtesy of B. Mascialino et al., INFN Genova

Radiotherapy with external beams, IMRT

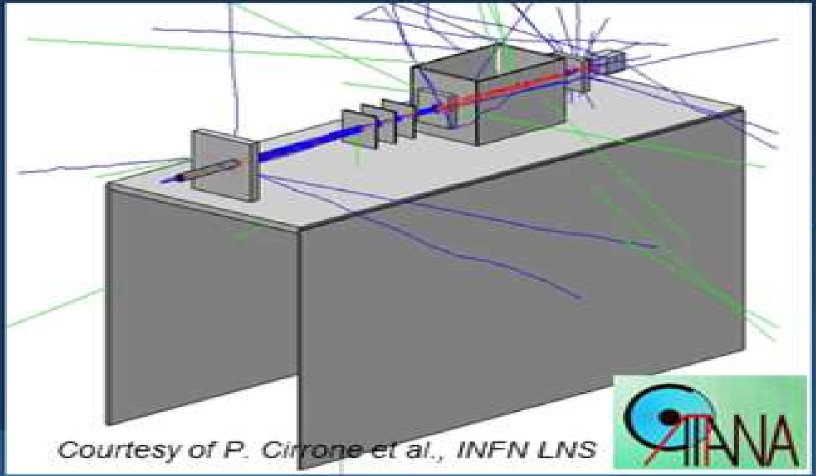

Courtesy of P. Cirrone et al., INFN LNS

Hadrontherapy

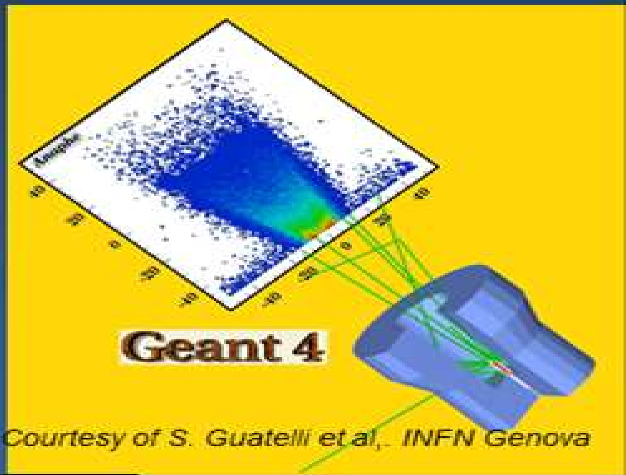

Brachytherapy

Courtesy of S. Guatelli et al,. INFN Genova

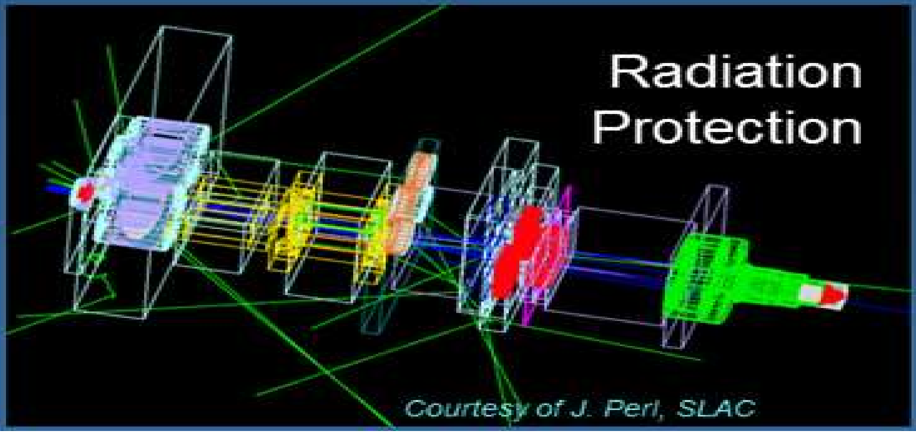

Radiation Protection

Courtesy of J. Perl, SLAC

Courtesy of L. Beaulieu et al., Laval

Materials and methods

Decay model

Week interaction: n → p + e^- + $\bar{\nu}_e$

In Geant4: *G4RadioactiveDecay()* provides:

- nuclear half-lives,
- nuclear level structure for the parent or daughter nuclide
- decay branching ratios
- the energy of the decay process.

These data taken from the Evaluated Nuclear Structure Data File (**ENSDF**) - National Nuclear Data Center - Brookhaven National Laboratory

Materials and methods

Decay model

G4RadioactiveDecay()

The shape of the energy spectrum of the emitted electron:

$$\frac{d^2n}{dEdp_e} = (E_0 - E_e)^2 E_e p_e F(Z, E_e) S(Z, E_0, E_e)$$

Where:

- E_0: Endpoint energy of decay, taken from ENSDF data
- E_e, p_e : Emitted electron energy and momentum
- Z: atomic number
- F: Fermi function $$F(\mathrm{Z}, E_e) = 2(1+\gamma)\,(2p_eR)^{2\gamma-2} e^{\pm\pi\alpha Z E_e/p_e} \frac{|\Gamma(\gamma + i\alpha Z E_e/p_e)|^2}{\Gamma(2\gamma+1)^2}$$
- S: Shape factor
  - R: nuclear radius
  - $\gamma = \sqrt{1-(\alpha Z)^2}$
  - α : fine structure constant
  - $|\Gamma(\gamma + i\alpha Z E_e/p_e)|^2$ computed using Wilkinson approximation

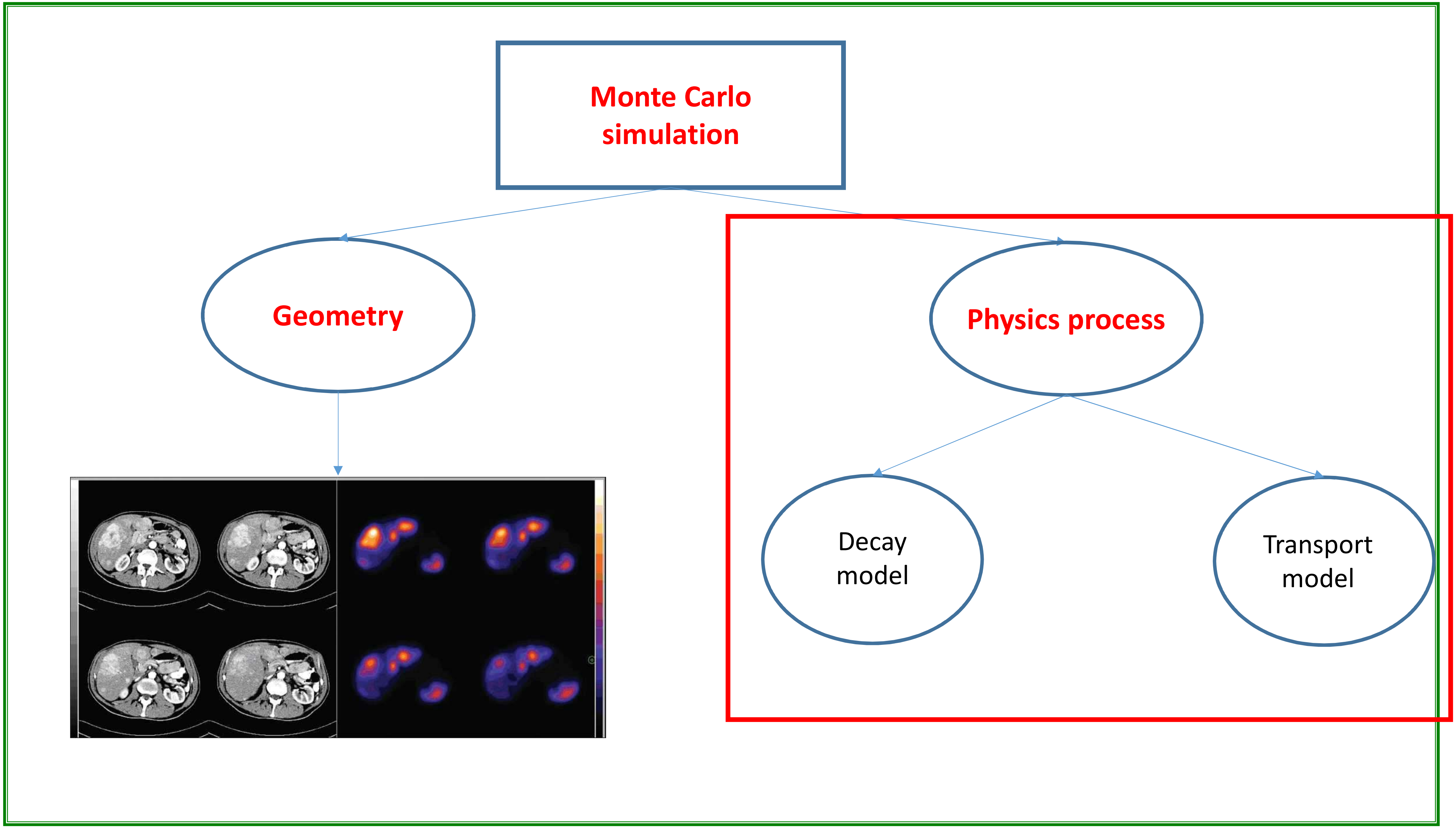

Monte Carlo simulation

Geometry

Physics process

Decay model

Transport model

Materials and methods

Transport model

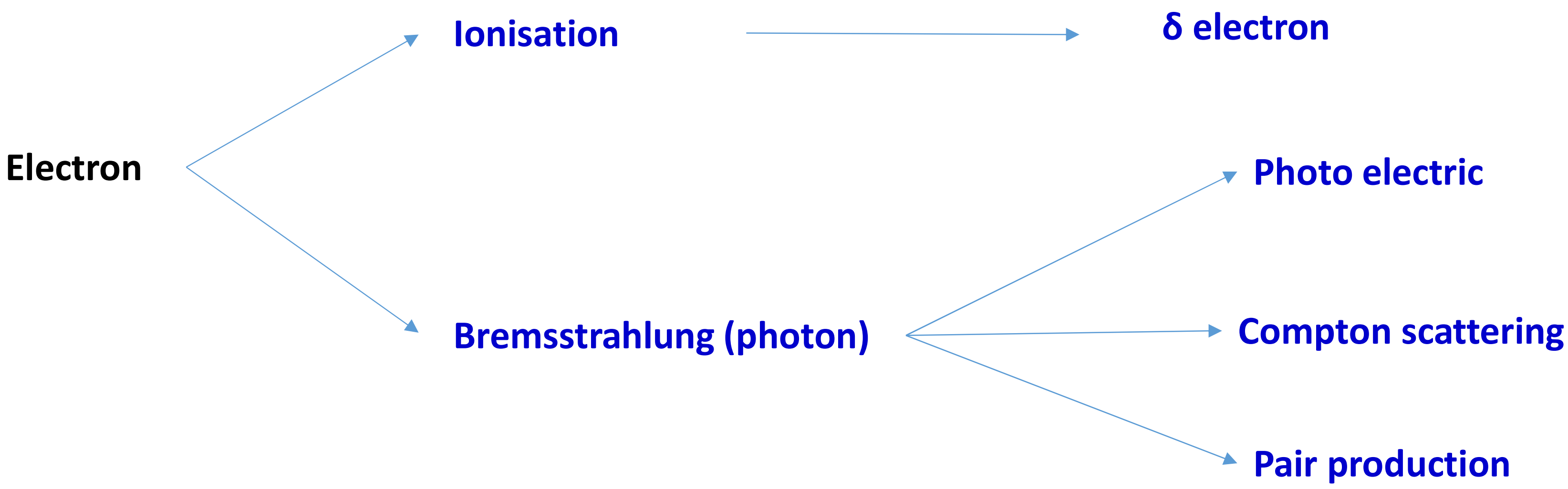

Electron

Ionisation

δ electron

Bremsstrahlung (photon)

Photo electric

Compton scattering

Pair production

Materials and methods

Transport model

G4LivermoreIonisation

- Shell structure
- Semi-empirical model, data from EEDL

Ex.:

$$\frac{dE}{dx} = \sum_{s}\left(\sigma_s(T)\frac{\int_{0.1e}^{Tc} t\,\frac{d\sigma}{dt}\,dt}{\int_{0.1eV}^{T_{max}}\frac{d\sigma}{dt}\,dt}\right)$$

- T: incident energy.
- T$_c$: secondary electron production threshold
- T$_{max}$ = 0.5T : maximum energy transferred to a secondary electron.
- $\sigma_s(T)$: total cross-section for the shell s at incident kinetic energy T

G4PenelopeIonisation

- Shell structure
- Based on Generalized Oscillation Strength (GOS) model

$$\boxed{\sigma^-(E) = \sigma_{dis,l} + \sigma_{dis,t} + \sigma_{clo}^-}$$

distant longitudinal

distant transverse

close interactions

$$\sigma_{dis,l} = \frac{2\pi e^4}{m_e v^2}\sum_{shells} f_k \frac{1}{W_k} ln\left(\frac{W_k}{Q_k^{min}}\frac{Q_k^{min} + 2m_e c^2}{W_k + 2m_e c^2}\right)\Theta(E - W_k)\Bigg)$$

m_e = mass of the electron;

v = velocity of the electron;

β = velocity of the electron in units of c;

f_k = number of electrons in the k-th atomic shell;

Θ = Heaviside step function;

W_k = resonance energy of the k-th atomic shell oscillator;

Q_k^{min} = minimum kinematically allowed recoil energy for energy transfer W_k

$$= \sqrt{\left[\sqrt{E(E+2m_ec^2)} - \sqrt{(E-W_k)(E-W_k+2m_ec^2)}\right]^2 + m_e^2c^4} - m_ec^2;$$

δ_F = Fermi density effect correction.

Materials and methods

Transport model

Most recommended: G4EmStandardPhysics_option4

➔ **Benchmark:**

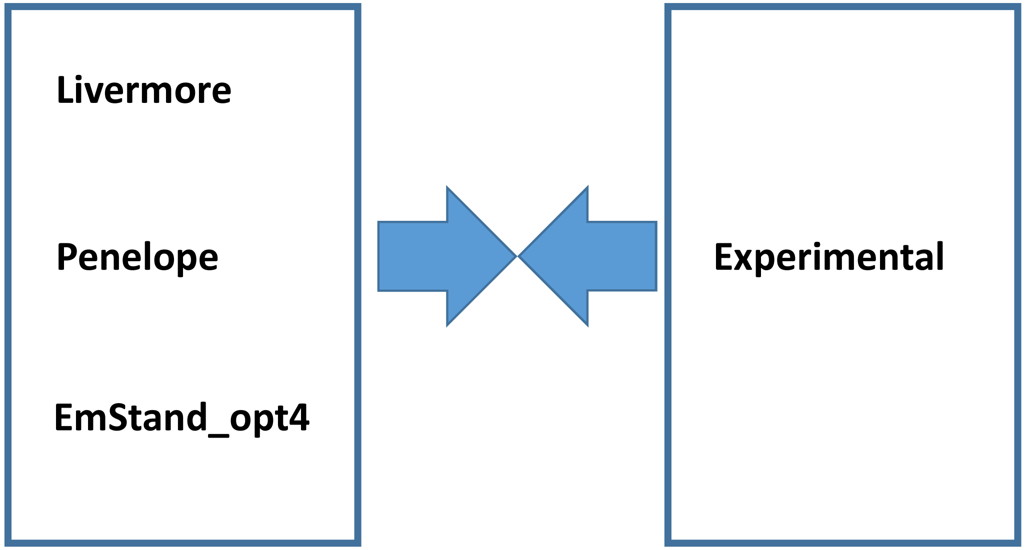

Livermore

Penelope

EmStand_opt4

Experimental

Materials and methods

Transport model

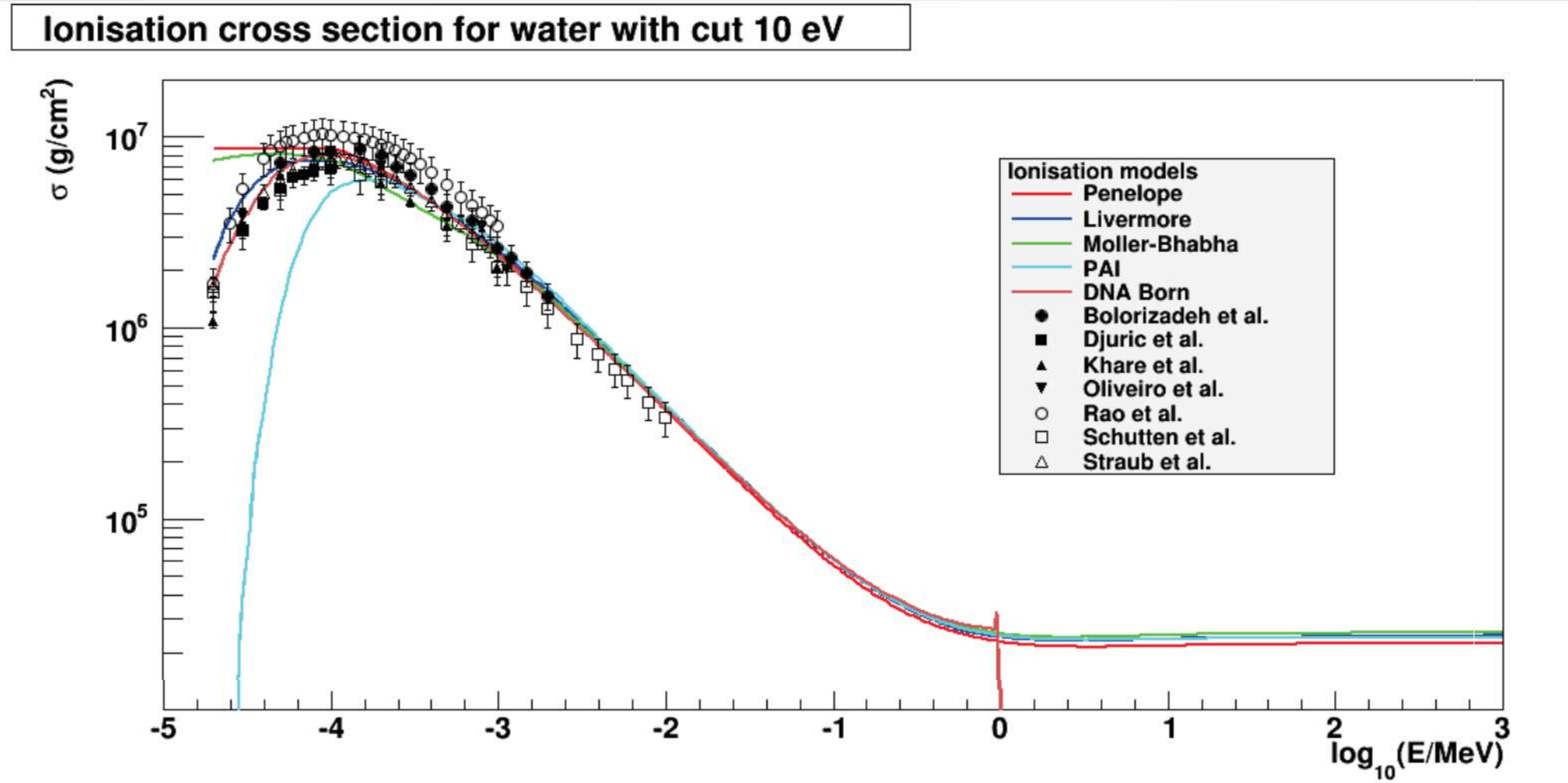

Source: V. Ivanchenko, CERN & Geant4 Associates International

Materials and methods

Transport model

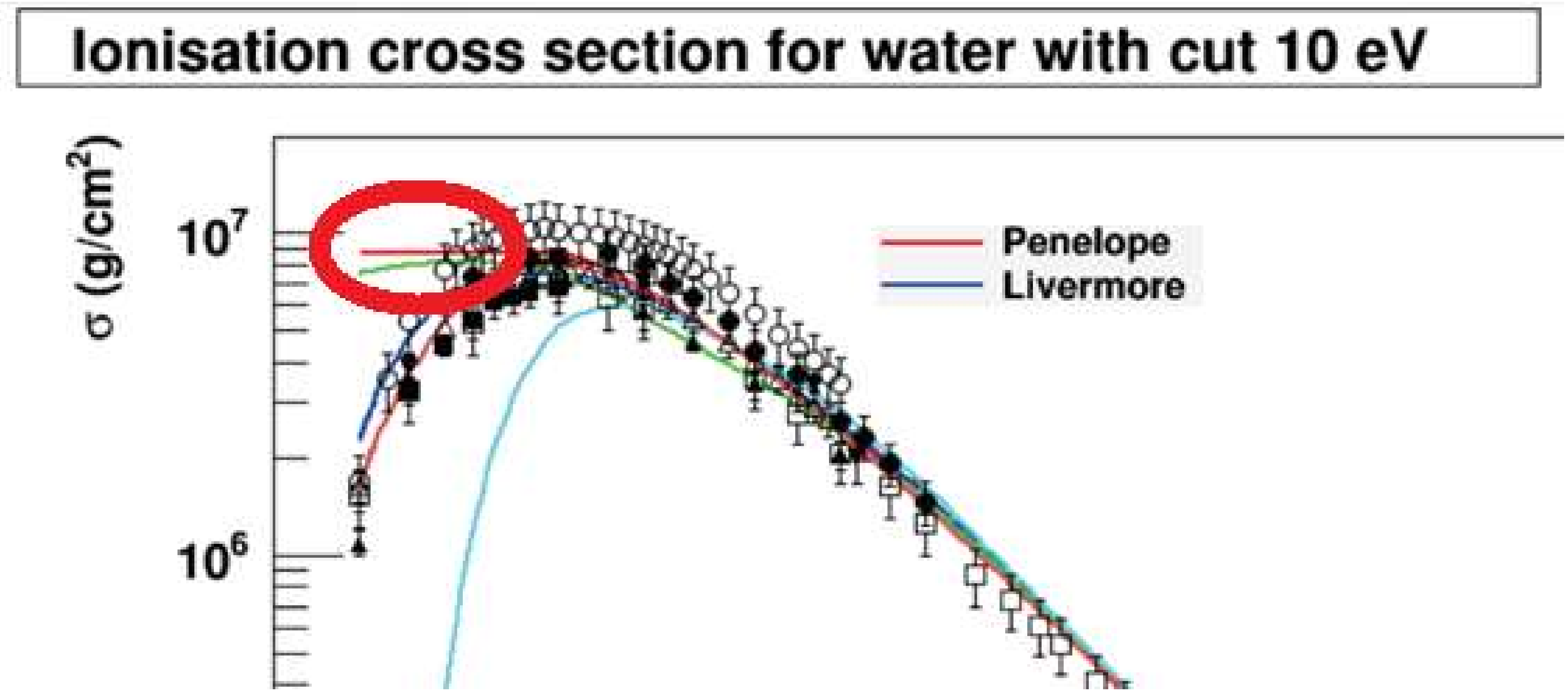

Materials and methods

Transport model

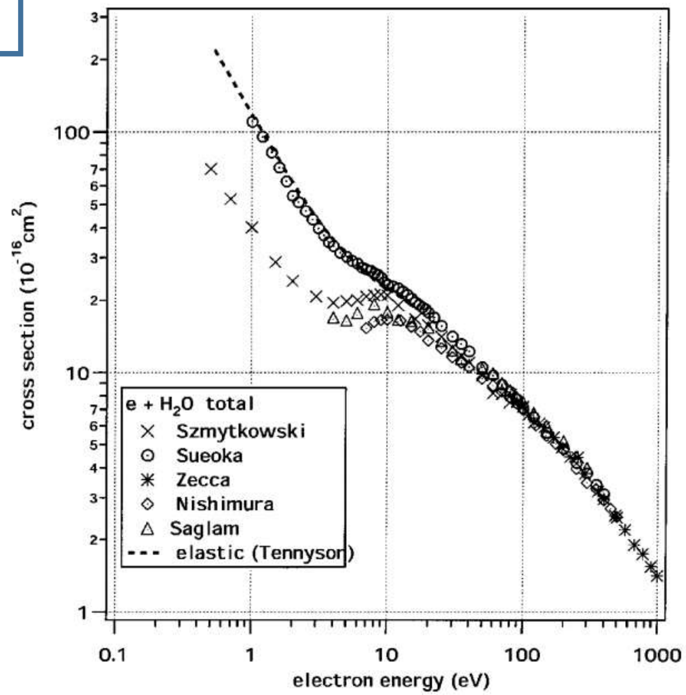

FIG. 2. Total scattering cross section, Q_T, of H_2O. A comparison is made of the experimental cross sections obtained by Szmytkowski (Ref. 21), Sueoka *et al.* (Ref. 26), Zecca *et al.* (Ref. 22), Nishimura and Yano (Ref. 23), and Saglam and Aktekin (Refs. 24 and 25). The theoretical elastic cross section obtained by Tennyson *et al.* (Ref. 28) is also shown for comparison.

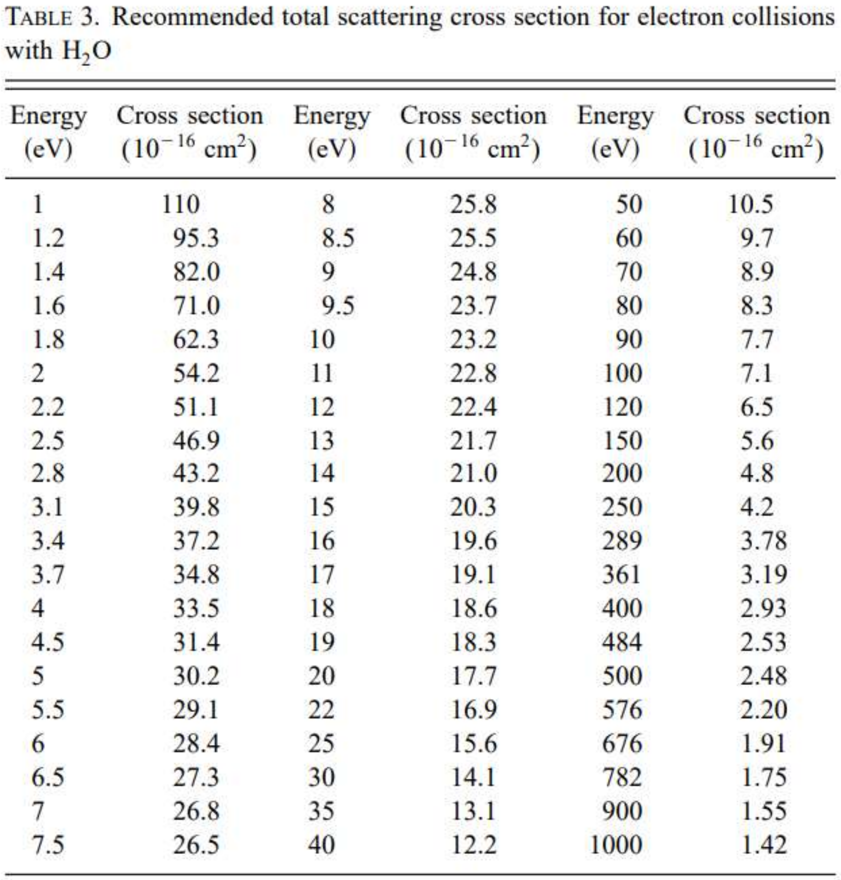

TABLE 3. Recommended total scattering cross section for electron collisions with H_2O

Energy (eV)	Cross section (10^{-16} cm^2)	Energy (eV)	Cross section (10^{-16} cm^2)	Energy (eV)	Cross section (10^{-16} cm^2)
1	110	8	25.8	50	10.5
1.2	95.3	8.5	25.5	60	9.7
1.4	82.0	9	24.8	70	8.9
1.6	71.0	9.5	23.7	80	8.3
1.8	62.3	10	23.2	90	7.7
2	54.2	11	22.8	100	7.1
2.2	51.1	12	22.4	120	6.5
2.5	46.9	13	21.7	150	5.6
2.8	43.2	14	21.0	200	4.8
3.1	39.8	15	20.3	250	4.2
3.4	37.2	16	19.6	289	3.78
3.7	34.8	17	19.1	361	3.19
4	33.5	18	18.6	400	2.93
4.5	31.4	19	18.3	484	2.53
5	30.2	20	17.7	500	2.48
5.5	29.1	22	16.9	576	2.20
6	28.4	25	15.6	676	1.91
6.5	27.3	30	14.1	782	1.75
7	26.8	35	13.1	900	1.55
7.5	26.5	40	12.2	1000	1.42

➔ Develope new semi-empirical model based on Livermore

Cross Sections for Electron Collisions with Water Molecules

Materials and methods

Transport model

How to validate?

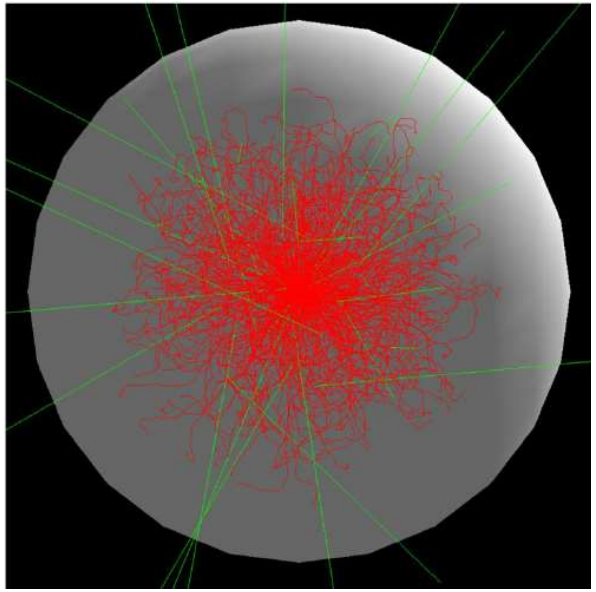

- Dose
- Cross section
- Mean free path
- …

Compare with experimental result published.

Applications and Perspectives

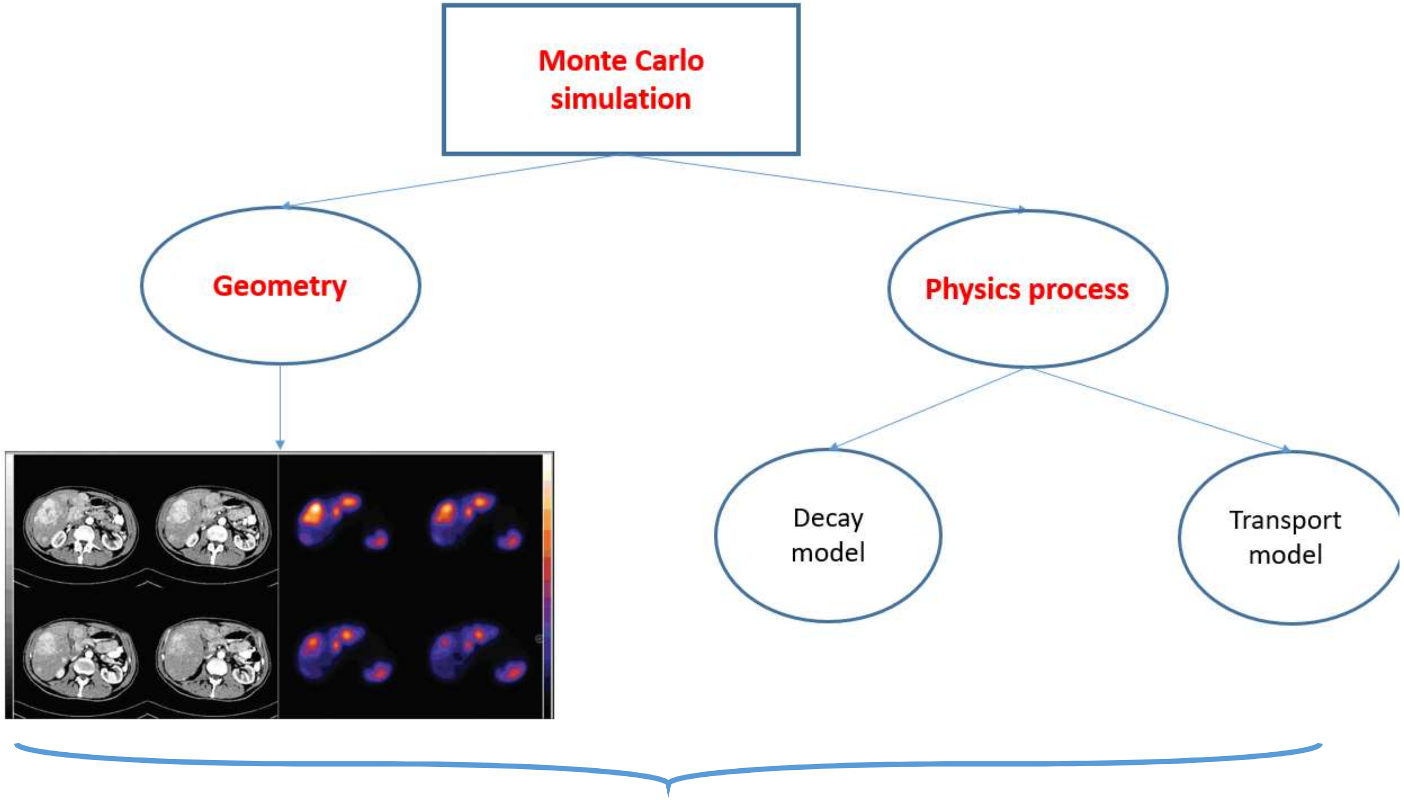

Monte Carlo simulation

Geometry

Physics process

Decay model

Transport model

-Calculate for several treatment cases

-Developing a platform

Comparision

This research

Simulation

Dose distribution

108 Military Hospital

post-treatment PET/CT scan

Dose distribution

Compare

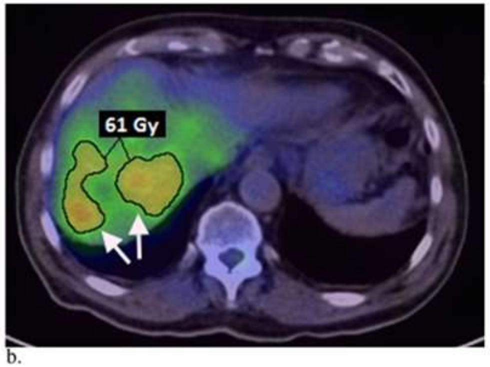

b.

Preliminary result

Preliminary result

Geometry constructed from DICOM CT of a patient treated in Hospital 108 (Vietnam)

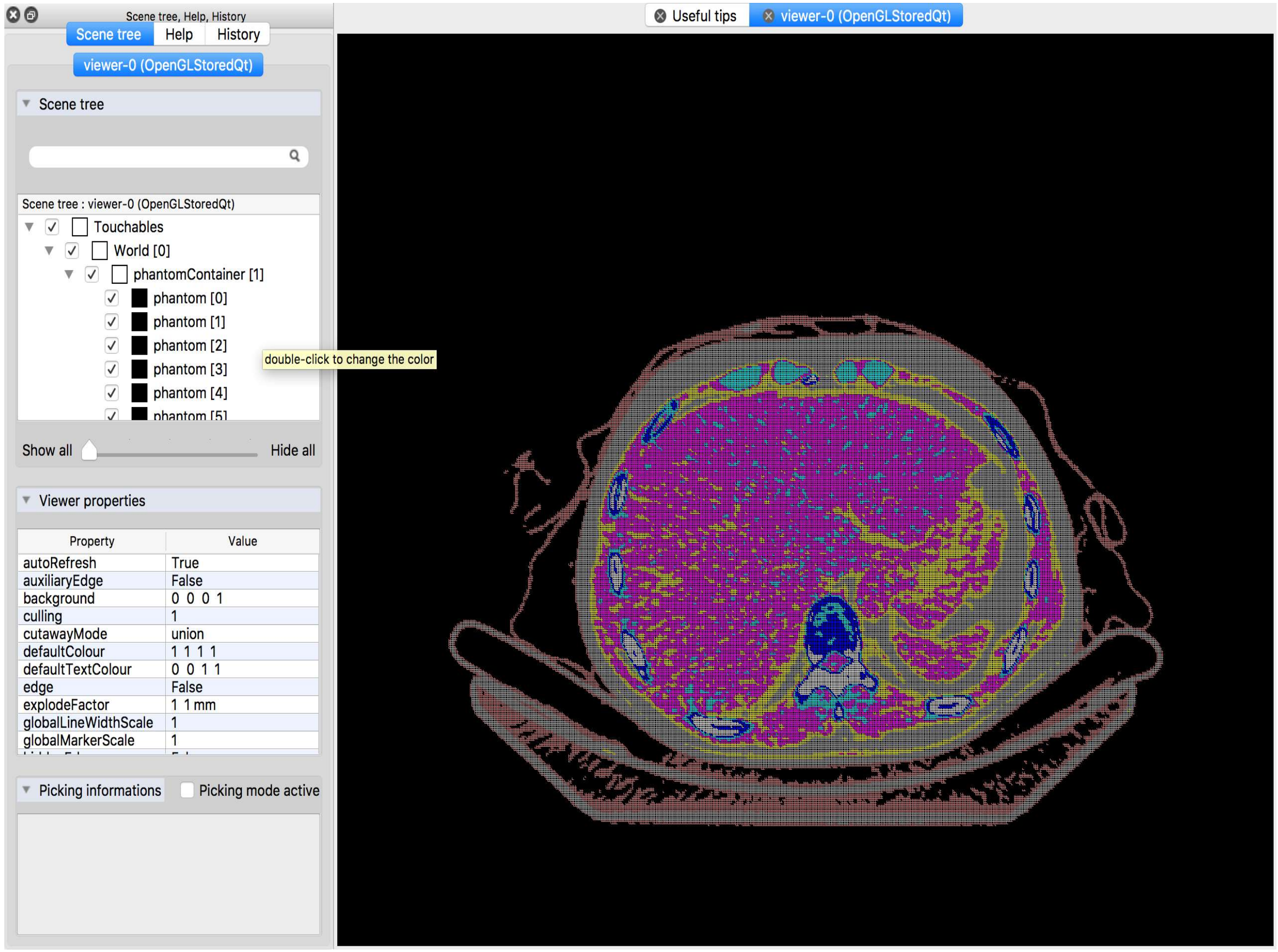

Property	Value
autoRefresh	True
auxiliaryEdge	False
background	0 0 0 1
culling	1
cutawayMode	union
defaultColour	1 1 1 1
defaultTextColour	0 0 1 1
edge	False
explodeFactor	1 1 mm
globalLineWidthScale	1
globalMarkerScale	1

Generate MAA distribution based on SPECT.

- Using ITK toolkit: itkImageSeriesReader class
- A new class implemented into G4 for generating MAA distribution

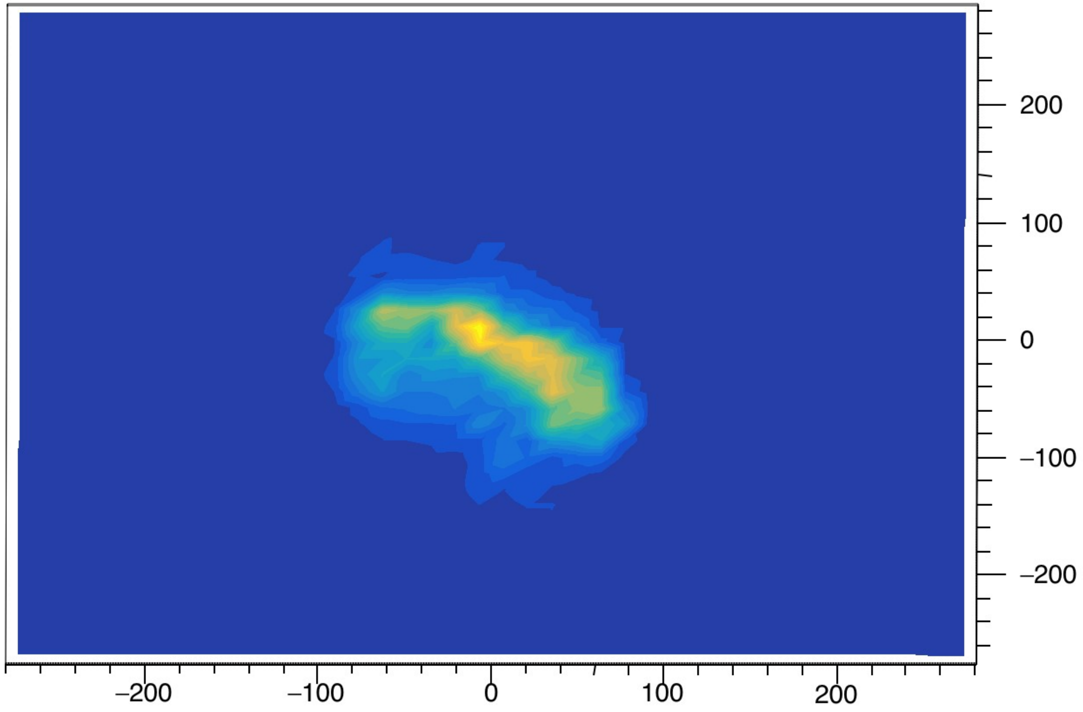

Preliminary result

Exported to **gdd** format for being displayed by gMocren

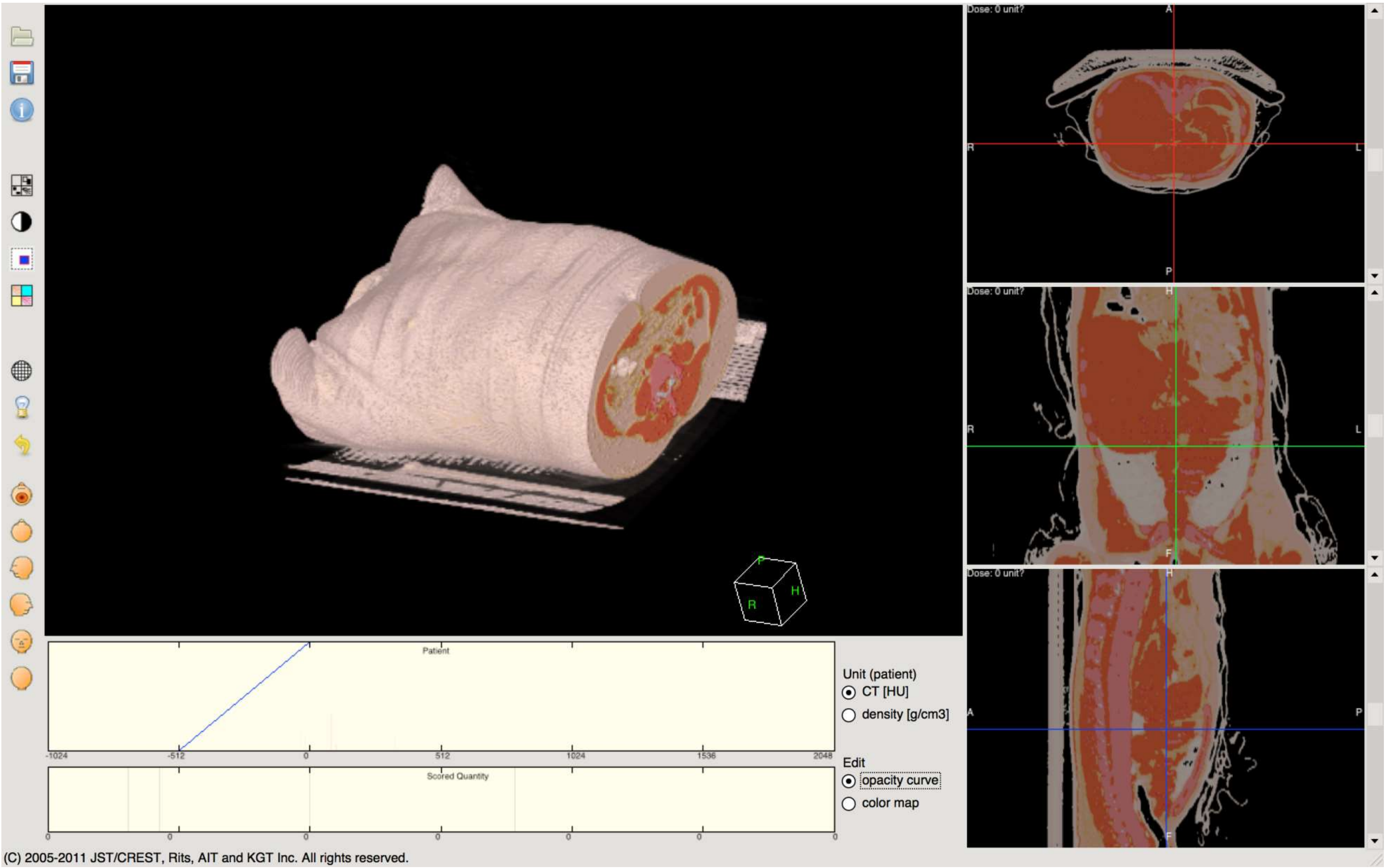

Unit (patient)
● CT [HU]
○ density [g/cm3]

Edit
● opacity curve
○ color map

(C) 2005-2011 JST/CREST, Rits, AIT and KGT Inc. All rights reserved.

THANK YOU FOR YOUR ATTENTION